

Elastic velocity models for gas-hydrate-bearing sediments—a comparison

Shyam Chand,¹ Tim A. Minshull,¹ Davide Gei² and José M. Carcione²

¹*School of Ocean and Earth Science, Southampton Oceanography Centre (SOC), European Way, Southampton SO14 3ZH, UK.*

E-mail: chand@soc.soton.ac.uk

²*Istituto Nazionale di Oceanografia e di Geofisica Sperimentale (OGS), Borgo Grotta Gigante 42c, 34010 Sgonico, Trieste, Italy*

Accepted 2004 June 16. Received 2004 May 5; in original form 2003 October 7

SUMMARY

The presence of gas hydrate in oceanic sediments is mostly identified by bottom-simulating reflectors (BSRs), reflection events with reversed polarity following the trend of the seafloor. Attempts to quantify the amount of gas hydrate present in oceanic sediments have been based mainly on the presence or absence of a BSR and its relative amplitude. Recent studies have shown that a BSR is not a necessary criterion for the presence of gas hydrates, but rather its presence depends on the type of sediments and the *in situ* conditions. The influence of hydrate on the physical properties of sediments overlying the BSR is determined by the elastic properties of their constituents and on sediment microstructure. In this context several approaches have been developed to predict the physical properties of sediments, and thereby quantify the amount of gas/gas hydrate present from observed deviations of these properties from those predicted for sediments without gas hydrate.

We tested four models: the empirical weighted equation (WE); the three-phase effective-medium theory (TPEM); the three-phase Biot theory (TPB) and the differential effective-medium theory (DEM). We compared these models for a range of variables (porosity and clay content) using standard values for physical parameters. The comparison shows that all the models predict sediment properties comparable to field values except for the WE model at lower porosities and the TPB model at higher porosities. The models differ in the variation of velocity with porosity and clay content. The variation of velocity with hydrate saturation is also different, although the range is similar. We have used these models to predict velocities for field data sets from sediment sections with and without gas hydrates. The first is from the Mallik 2L–38 well, Mackenzie Delta, Canada, and the second is from Ocean Drilling Program (ODP) Leg 164 on Blake Ridge. Both data sets have V_p and V_s information along with the composition and porosity of the matrix. Models are considered successful if predictions from both V_p and V_s match hydrate saturations inferred from other data. Three of the models predict consistent hydrate saturations of 60–80 per cent from both V_p and V_s from log and vertical seismic profiling data for the Mallik 2L–38 well data set, but the TPB model predicts 20 per cent higher saturations, as does the DEM model with a clay–water starting medium. For the clay-rich sediments of Blake Ridge, the DEM, TPB and WE models predict 10–20 per cent hydrate saturation from V_p data, comparable to that inferred from resistivity data. The hydrate saturation predicted by the TPB model from V_p is higher. Using V_s data, the DEM and TPB models predict very low or zero hydrate saturation while the TPB and WE models predict hydrate saturation very much higher than those predicted from V_p data. Low hydrate saturations are observed to have little effect on V_s . The hydrate phase appears to be connected within the sediment microstructure even at low saturations.

Key words: Blake Ridge, effective medium, gas hydrate, hydrate saturation, Mallik well, velocity.

1 INTRODUCTION

Gas hydrate is a naturally occurring solid composed of water molecules in a rigid lattice of cages, with most cages containing a molecule of natural gas, mainly methane (Brooks *et al.* 1986; Kvenvolden 1998; Kastner *et al.* 1998). Although three crystalline structures, I, II and H, have been recognized for gas hydrates in nature, structure I (which contains methane only) is most common (Kvenvolden 2000). Other structures normally contain higher-order hydrocarbons such as ethane along with methane (Brooks *et al.* 1986; Davidson *et al.* 1986; Sassen & MacDonald 1994). Gas hydrates are widespread in seafloor sediments along continental margins, and in permafrost regions. They occur in finely disseminated, nodular, layered or massive forms (Malone 1985; Sloan 1990; Kvenvolden 2000). Gas hydrates may be detected in seismic reflection data as bottom simulating reflectors (BSRs), with high-amplitude and reversed polarity, which are subparallel to the seabed and are interpreted to mark the base of the gas hydrate stability zone (GHSZ) (Shipley *et al.* 1979). The presence of gas hydrates is also inferred from the observation of gas escape and fluid flow features such as pockmarks, pipes, acoustic maskings and acoustic turbidity in seismic sections (e.g. Chand & Minshull 2003). Seismic and drilling studies in hydrate provinces have demonstrated that BSRs are normally underlain by free gas (Singh *et al.* 1993; Mackay *et al.* 1994; Holbrook *et al.* 1996; Collett *et al.* 1999). Where no direct measurements are available, detailed knowledge of the compressional and/or shear wave velocity distribution in marine sediments may be used to derive quantitative estimates of gas hydrate and free gas in the pore space (e.g. Lee *et al.* 1996; Ecker *et al.* 2000; Jakobsen *et al.* 2000).

Higher velocities than those of water-filled, normally compacted marine sediments can often be attributed to the presence of gas hydrate. Such anomalies can be used to infer the concentration of hydrate if the relationship between velocity and gas hydrate content is known. Several theoretical approaches have been developed to predict this relationship. All of them are in principle effective medium approaches in which the physical properties of the composite sediment with or without hydrate are calculated by mixing the various components in different ways.

With several different published methods available, it is not clear which the geophysicist should use to interpret seismically determined velocities. We have made a general comparison of the most widely used effective-medium methods, using a consistent set of parameters for the properties of the component materials, and applied them to some of the most comprehensive borehole data sets available. Our aim is to assess objectively which methods give the most reliable results for a range of sediment types. The two data sets chosen include both compressional and shear wave velocity (V_p and V_s) measurements. The data sets are borehole measurements from clay-rich sediments in the Blake Ridge area (Guerin *et al.* 1999) and sand-rich sediments in the Mackenzie Delta area (Goldberg *et al.* 2000). The theories compared are the empirical weighted equation (WE) of Lee *et al.* (1996), a three-phase effective-medium theory (TPEM) (Ecker *et al.* 1998; Helgerud *et al.* 1999; Ecker *et al.* 2000), a three-phase Biot theory (TPB) (Carcione & Tinivella 2000; Gei & Carcione 2003) and an approach using differential effective-medium theory (DEM) (Jakobsen *et al.* 2000) (Fig. 1).

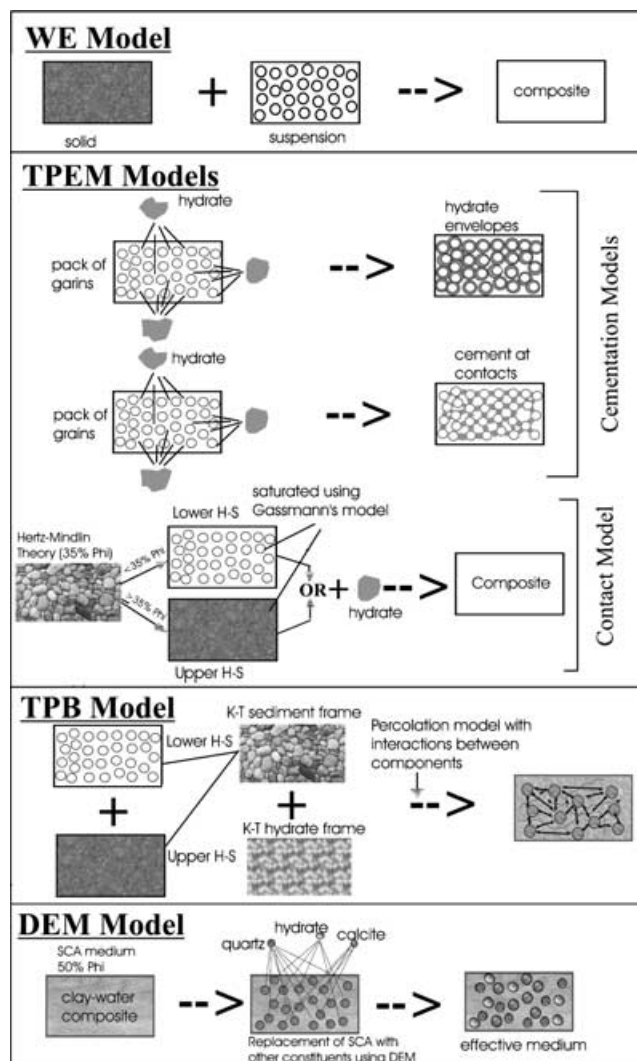


Figure 1. Diagram illustrating the theory behind effective-medium models. The WE model is an average of equations for solids and suspensions. TPEM cementation models represent the addition of hydrate as cement to a composite material through laws of cementation, while in the contact model hydrate contributes to matrix properties through laws bounding physical properties. The TPB model defines the interaction of different components of the composite with each other through a percolation theory, and the DEM model uses laws of bi-connected aggregates. (K–T is Krief's theory; Krief *et al.* 1990).

2 ELASTIC VELOCITY MODELS

2.1 Weighted equation (WE)

Lee *et al.* (1996) estimated the P -wave velocity of hydrate-bearing sediment from a weighted average of the three-phase Wood equation (Wood 1941) and the three-phase time-average equation (Wyllie *et al.* 1958) (Fig. 1). The parameters involved are the concentration of hydrate in the pore space S , the porosity ϕ , a weighting factor W and a constant n that simulates the rate of lithification with hydrate concentration. The weight W is estimated from the V_p of non-gas-hydrate-bearing sediments and the exponent n is adjusted to match

the gas hydrate concentrations estimated independently from V_p and V_s . The S -wave velocity is calculated from V_p , S , ϕ and the P to S velocity ratios for the matrix and hydrate. A value of $W > 1$ and low n favours the Wood equation, which is valid for particles in suspension; a value of $W < 1$ and high n favours the time-average equation, which is more appropriate for consolidated sediments.

The main advantages of the weighted equation are that it is simple and that the parameters W and n can be adjusted to fit a given data set. However, there is no physical meaning to the weighted average and the model requires a substantial data set to constrain these parameters. Since W and n are derived empirically, the approach can be applied only to data sets where the sediments are of similar type to those used to determine them. Also, variables such as effective pressure and particle aspect ratio and size are not considered at all, and the approach is unable to handle anisotropy. V_s is estimated from V_p through an empirical relation, so it is difficult to treat by this method the change in V_s produced when hydrate starts contributing to the strength of the sediment frame.

2.2 Three-phase effective-medium theory (TPEM)

Ecker *et al.* (1998) considered two mechanically extreme cases of hydrate morphology. In the first model (the 'cementation model'), hydrate cements the sediment either at the grain boundaries or by enveloping whole grains, while in the second model (the 'contact model'), hydrate is located away from grain contacts and does not affect the strength of the sediment (Dvorkin & Nur 1996) (Fig. 1). In the latter case hydrate can be considered either as part of the pore fluid or as part of the solid sediment (Ecker *et al.* 1998, 2000).

The cementation model is based on the theory of Dvorkin *et al.* (1991, 1994), Dvorkin & Nur (1996) and Ecker *et al.* (1998), and predicts the normal and shear stiffness of a two-grain combination with elastic cement at the contact. The grain contact model uses Hertz–Mindlin theory (Mindlin 1949) to calculate the moduli at critical porosity (35–40 per cent, Nur *et al.* 1998), the porosity at which a granular composite with spherical grains ceases to be a suspension and becomes grain supported. Modified Hashin–Shtrikman (H–S) bounds (Dvorkin & Nur 1996) are then used to calculate the dry rock moduli at all porosities from this initial model (Ecker *et al.* 2000). The moduli thus obtained depend on the effective pressure, the bulk modulus, the shear modulus and the Poisson ratio of the composite sediment and the average number of contacts per grain in the sphere pack m , estimated as 8–10 (Murphy 1982; Dvorkin & Nur 1996; Ecker *et al.* 2000).

For the grain contact model if hydrate is considered as part of the fluid, the shear modulus is independent of hydrate saturation and the bulk modulus is calculated from the Reuss average of the bulk moduli of hydrate and pore fluid (Fig. 1). If hydrate is considered as part of the solid, both bulk and shear moduli are calculated from the Reuss average of the bulk moduli of sediment, hydrate and pore fluid, and the Reuss average of the shear moduli of sediment and hydrate. The effective pressure used in Hertz–Mindlin theory is taken as the difference between the lithostatic and hydrostatic pressure. For a mixed mineralogy, the dry rock moduli are calculated from those of individual components using the average of Hill (1952), also known as the Voigt–Reuss–Hill average (VRH). Once dry rock moduli have been determined, the equation of Gassmann (1951) is used to estimate the saturated rock moduli for all the models.

The velocities predicted by the cementation model are much higher than those normally observed in nature (Ecker *et al.* 1998). The velocities predicted by this model increase steeply with only a small addition of hydrate to the sediment (Figs 2a,b,e and f). If

hydrate envelopes sediment grains, the model appears to predict unphysical results with P and S velocities increasing with porosity at porosities below ~60 per cent (Figs 2b and f). The S -wave velocity of the cementing model with hydrate at contacts shows a similar effect at low porosities (Fig. 2e). The grain contact model with hydrate as a part of the solid predicts P -wave velocities that are 30–40 per cent lower. If hydrate is assumed to form part of the pore fluid, the model predicts that V_s is independent of hydrate saturation (Figs 2c and g), in contrast to observations in areas of high hydrate saturation (e.g. Collett *et al.* 1999). The increase in V_p with hydrate saturation is also much less than is observed. The contact model requires an assumption about the number of contacts per grain, which varies between 8 and 12 depending on the size and shape of the grains, and varies strongly with clay content (Marion *et al.* 1992; Blangy *et al.* 1993). Finally, the anisotropic effects of clay particle alignment are not accounted for by this approach.

2.3 Three-phase Biot theory (TPB)

Carcione & Tinivella (2000) and Gei & Carcione (2003) developed an approach based on those of Leclaire *et al.* (1994), who applied Biot theory to partially frozen porous media, and of Santos *et al.* (1990a,b), who described wave propagation in a porous medium saturated with a mixture of two immiscible, viscous, compressible fluids (Fig. 1). The approach of Leclaire *et al.* (1994) assumes that there is no direct contact between solid grains and ice (or equivalently, hydrate), since in principle water tends to form a thin film around the grains. Carcione & Tinivella (2000) added contributions to the potential and kinetic energies due to the contact between the solid grains and the hydrate, and to the stiffening of the skeleton due to grain cementation. The shear modulus is also changed by cementation of the grains by hydrate. The interaction between the grain and hydrate phases is described by 'tortuosity' terms. These terms give the difference between the microvelocity field (the flow of hydrate through the matrix) and the macrovelocity field (the flow of the matrix through hydrate), and these terms vanish for rigid solids. When the sediment is unconsolidated, however, these terms contribute to the kinetic energy. Although Biot theory neglects contributions to the kinetic energy from interactions between the solid and the pore fluid, Carcione & Tinivella (2000) add a frequency-dependent term describing the transmission of shear deformation from one matrix to the other through a very thin and viscous water layer.

Gei & Carcione (2003) generalized this theory to include the effects of pore pressure, partial saturation (gas and water) and the presence of dissipation mechanisms. The effective pressure term given by Carcione & Tinivella (2000) is modified by multiplying it by an effective stress coefficient, an empirical parameter derived from laboratory data sets (Todd & Simmons 1972; Zimmerman & King 1986). The model yields seismic velocities as a function of hydrate concentration, porosity, saturation, dry-rock moduli and fluid and solid grain properties. The moduli of the dry rock and of the hydrate matrix are estimated using the model of Krief *et al.* (1990). The porosity dependence of these moduli is assumed to be consistent with the concept of critical porosity, and is determined by an empirical coefficient. Calibration of the model is required using either borehole log, vertical seismic profiling or laboratory data to estimate the various empirical coefficients involved. The pressure dependence of the dry frame modulus is taken care of using an effective stress law.

A similar approach based on Biot and Gassmann theories is proposed by Lee (2002), who assumes that the S to P velocity ratio of

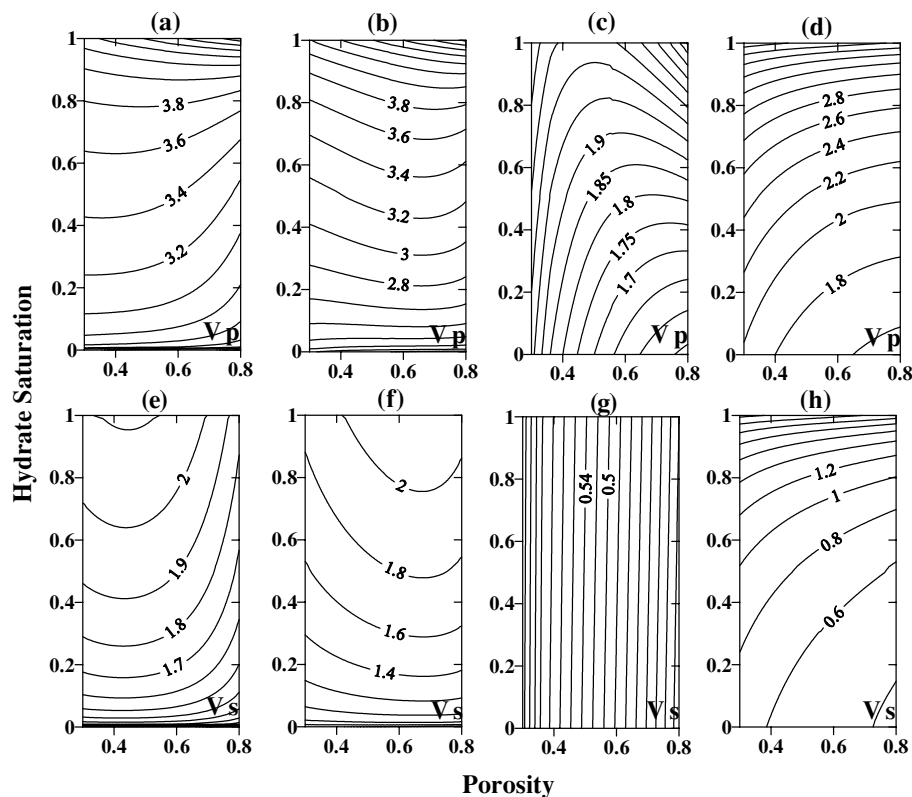


Figure 2. Contour plots of V_p and V_s as functions of hydrate saturation and porosity at 50 per cent clay content for different TPME models (Ecker *et al.* 1998, 2000; Helgerud *et al.* 1999). Contours are labelled in km s^{-1} : (a) V_p for the cementation model with hydrate at grain boundaries, (b) V_p for the cementation model with hydrate enveloping grains, (c) V_p for the contact model with hydrate in the fluid, (d) V_p for the contact model with hydrate as part of the solid grains, (e) V_s for the cementation model with hydrate at grain boundaries, (f) V_s for the cementation model with hydrate enveloping the grains, (g) V_s for the contact model with hydrate in the fluid, (h) V_s for the contact model with hydrate as part of the solid grains.

the sediment is proportional to the S to P velocity ratio of the matrix and its porosity. But this assumption may fail at higher porosities as V_s/V_p of the sediment approaches zero as porosity approaches 100 per cent. The Biot coefficient has to be derived using the WE or TPME model, so Lee's results have the problems discussed above that arise from the use of empirical relations or of Hashin–Shtrikman and Hertz–Mindlin theories.

2.4 Differential effective-medium theory (DEM)

Jakobsen *et al.* (2000) relate the seismic properties of clay-rich hydrate-bearing sediments to their porosity, mineralogy, microstructure, clay particle anisotropy and hydrate saturation, following approaches developed by Hornby *et al.* (1994) and by Sheng (1990) (Fig. 1). Of the four approaches we compare here, this is the only one that explicitly incorporates the effects of anisotropy due to clay fabric. The building blocks are considered to be transversely isotropic due to the alignment of clay platelets, and the theory is based on a combination of a self-consistent approximation (SCA) (Willis 1977), a differential effective-medium (DEM) theory (Nishizawa 1982) and a method of smoothing for crystalline aggregates (Bonilla & Keller 1985). The model structure consists of inclusions embedded in a homogeneous matrix; the effective elastostatic parameters can then be expressed in terms of a tensor K_{ijkl} which relates the applied stress to the average strain in each inclusion (Hudson 1991). The model starts with a self-consistent method in which K_{ijkl} is determined approximately using a single inclusion in a host having the elastic properties of the yet to be determined effective medium

(Hornby *et al.* 1994). These individual components are then replaced with an effective material. Starting with such a bi-connected medium created with a self-consistent approximation, which is valid only for porosities below 60 per cent, the stiffness values at other porosities are calculated by successive operations of removing an infinitesimal subvolume of host material and replacing it with another component through DEM theory (Nishizawa 1982).

Since the DEM theory preserves the connectivity of the phases (Sheng 1990), this procedure produces a sediment that is bi-connected at all porosities. The material is considered to be made of blocks of fully aligned composite but arranged in different orientations. A limitation of this approach is that it will not take into account the weaker bonding and greater compliance likely to exist at the edges of the individual domains of preferential particle alignment (Bennett *et al.* 1991). The effective stiffness is calculated using the Voigt–Reuss–Hill average (Hill 1952) followed by a ‘method of smoothing’ (Bonilla & Keller 1985) which can be used to calculate the effects of interactions between neighbouring grains, thus minimizing the error due to effects at edges when the orientation of individual components is different. A further limitation of DEM theory is that pressure effects are not considered other than through resulting changes in porosity.

2.5 Comparison

In order to objectively compare the approaches described, we require a consistent set of input parameters. A set of values for the physical constants used by the models is given in Table 1. A variety of values

Table 1. Parameters used in the models.

| Parameter | Value |
|--|---|
| Critical porosity, ϕ_c | 0.35 (Nur <i>et al.</i> 1998) |
| Quartz bulk modulus | 36 GPa (Carmichael 1982) |
| Quartz shear modulus | 45 GPa (Carmichael 1982) |
| Quartz density | 2650 kg m ⁻³ (Carmichael 1982) |
| Clay bulk modulus | 20.9 GPa (Mavko <i>et al.</i> 1998) |
| Clay shear modulus | 6.85 GPa (Mavko <i>et al.</i> 1998) |
| Clay density | 2580 kg m ⁻³ (Hornby <i>et al.</i> 1994) |
| Hydrate bulk modulus | 7.7 GPa (Waite <i>et al.</i> 2000) |
| Hydrate shear modulus | 3.2 GPa (Waite <i>et al.</i> 2000) |
| Hydrate density | 910 kg m ⁻³ (Waite <i>et al.</i> 2000) |
| Water bulk modulus | 2.32 GPa (Carmichael 1982) |
| Water density | 1030 kg m ⁻³ |
| Viscosity of water | 2.04×10^{-3} Pa s |
| Viscosity of gas | 1.34×10^{-5} Pa s |
| Parameter describing the shape of the pore network | 8 |
| Average number of contacts per grain | 10 (Murphy 1982) |
| Weighting factor, W | 1.0 |
| Compaction parameter, n | 1.0 |
| Aspect ratio for clay | 1/20 |

of physical constants are used in the literature. In particular, some authors have used constants for structure II hydrates; here we use values for structure I hydrates since these are observed to occur more widely in nature (Kvenvolden 2000). Similarly the quoted moduli of clay particles also vary widely between different publications; the values used here are from Mavko *et al.* (1998) and are based on measurements on low-porosity clays and projected to zero porosity.

A problem with the WE model (Lee *et al.* 1996) is that the additional parameters W and n have little physical meaning. The parameter n should vary with hydrate content if it represents lithification, but in fact is normally fixed as $n = 1$. The value for W of 1.44 used by Lee & Collett (2001) for data from the Mallik 2L–38 well in the Mackenzie Delta, Canada, implies preferential use of the Wood equation, appropriate for suspensions, yet the data come from consolidated sediment at 640–1100 m depth from a permafrost region. A problem with the grain contact TPTEM models is that all solid grains, including clay particles, are assumed to be spherical, which seems unlikely based on the observations of seismic anisotropy in clay-rich sediments (e.g. Pecher *et al.* 2003).

The presence of clay lowers pore aspect ratios, and this justifies the usage in the DEM model of ellipsoidal fluid inclusions whose aspect ratio distribution depends on the clay content (Eastwood & Castagna 1983; Xu & White 1995). A recent study using walk-away vertical seismic profiling (VSP) data in the Blake Ridge area also reported anisotropy due to clay particle alignment (Pecher *et al.* 2003). The critical porosity depends strongly on the clay content (Marion *et al.* 1992; Blangy *et al.* 1993), so the TPTEM approach is limited if a constant 35 per cent critical porosity is assumed (Ecker *et al.* 1998; Helgerud *et al.* 1999).

Additional parameters required by the TPB approach are the pore fluid viscosities, the shape of the network, the radii of grains and capillary spaces and the permeability of the solid and hydrate matrix. When laboratory or VSP data are not available for calibration, the moduli of the rock frame are calculated using the Hashin–Shtrikman bounds and the theory of Krief *et al.* (1990).

The DEM approach requires a clay particle orientation distribution which should be based on measurements of real samples, but otherwise all other parameters are physical constants. A limitation of this approach is that quartz, calcite and hydrate grains are added

as inclusions and will not affect the strength of the composite, an assumption that may fail in the case of sediment with a low clay content. Hydrate can be added as a part of the load-bearing framework by starting with application of the self-consistent approximation to a clay–hydrate composite.

3 MODEL PREDICTIONS

We analysed the theoretical models described above for variation of V_p and V_s with clay content, porosity and hydrate saturation and also assessed the influence of various model assumptions, using the physical constants of Table 1. For the anisotropic DEM model we used the clay particle orientation distribution of Jakobsen *et al.* (2000), while for the isotropic model we used a uniform distribution. In both cases we used a clay–water composite as the starting medium in the self-consistent approximation. The TPTEM model used for comparison is the contact model with hydrate as a part of solid, because this model appears to give the most realistic results (Ecker *et al.* 2000). The effective pressure value for the Hertz–Mindlin theory is calculated as the difference between lithostatic and hydrostatic pressure for 200 m of sediment lying beneath 1000 m of water.

The P -wave velocities differ between models, particularly the rate of change of velocity with porosity. First, we consider a saturated sample containing clay and quartz only. The velocity predicted by the WE model ranges from 2.0 km s⁻¹ at 30 per cent porosity and 20 per cent clay content to just over 1.5 km s⁻¹ at 80 per cent porosity and 70 per cent clay content (Fig. 3a). Similarly for the TPTEM model the velocity decreases from 2.5 to 1.5 km s⁻¹ (Fig. 3b). For the TPB model the pattern is entirely different, with the velocity decreasing from 2.3 to 1.5 km s⁻¹ at 60 per cent porosity and then flattening at this porosity without any further decrease (Fig. 3c). The isotropic DEM model predicts a decrease of V_p from ~ 2.5 km s⁻¹ at 30 per cent porosity to ~ 1.5 km s⁻¹ at 80 per cent porosity (Fig. 3d). For the transversely isotropic models the vertical velocity ranges between 2.1 and 1.5 km s⁻¹ (Fig. 3e) and the horizontal velocity ranges between 2.4 and 1.5 km s⁻¹ (Fig. 3f). In contrast to the other models and to experimental data (Goldberg & Gurevich 1998), the DEM model predicts an increase of velocity with clay content (Figs 3e and f). The predicted increase can be attributed to the effect of clay–water connectivity assumed in the initial self-consistent approximation, which is preserved even at low clay content and overrides the effect of the higher elastic modulus of quartz. This behaviour illustrates a limitation of the DEM model and is due to the fact that only the starting mineral grain in the SCA medium is assumed to be fully connected, even at low concentrations. Anisotropy also increases with clay content, with large differences between horizontal and vertical velocity predicted at high clay contents (Figs 3e and f).

The predicted S -wave velocity also varies dramatically between models (Fig. 4). The WE model ranges predict values decreasing from 0.86 to 0.22 km s⁻¹ as clay content and porosity increase (Fig. 4a). The TPTEM model predicts a similar variation, from 1.1 to 0.2 km s⁻¹ (Fig. 4b), while the TPB model predicts a decrease from 1.1 to 0.1 km s⁻¹ at ~ 55 per cent porosity and no change with porosity above this value (Fig. 4c). The S -wave velocity predicted by the isotropic DEM model ranges between 1.0 and 0.15 km s⁻¹ (Fig. 4d), and like V_p increases with clay content. The transverse isotropic model predicts a range of 0.95–0.15 km s⁻¹ for vertical V_s and 1.1–0.2 km s⁻¹ for the horizontal V_s (Figs 4e and f). Thus, although the DEM, TPTEM and TPB models all show a similar variation of S -wave velocities, the dependence on clay content and porosity varies significantly between them.

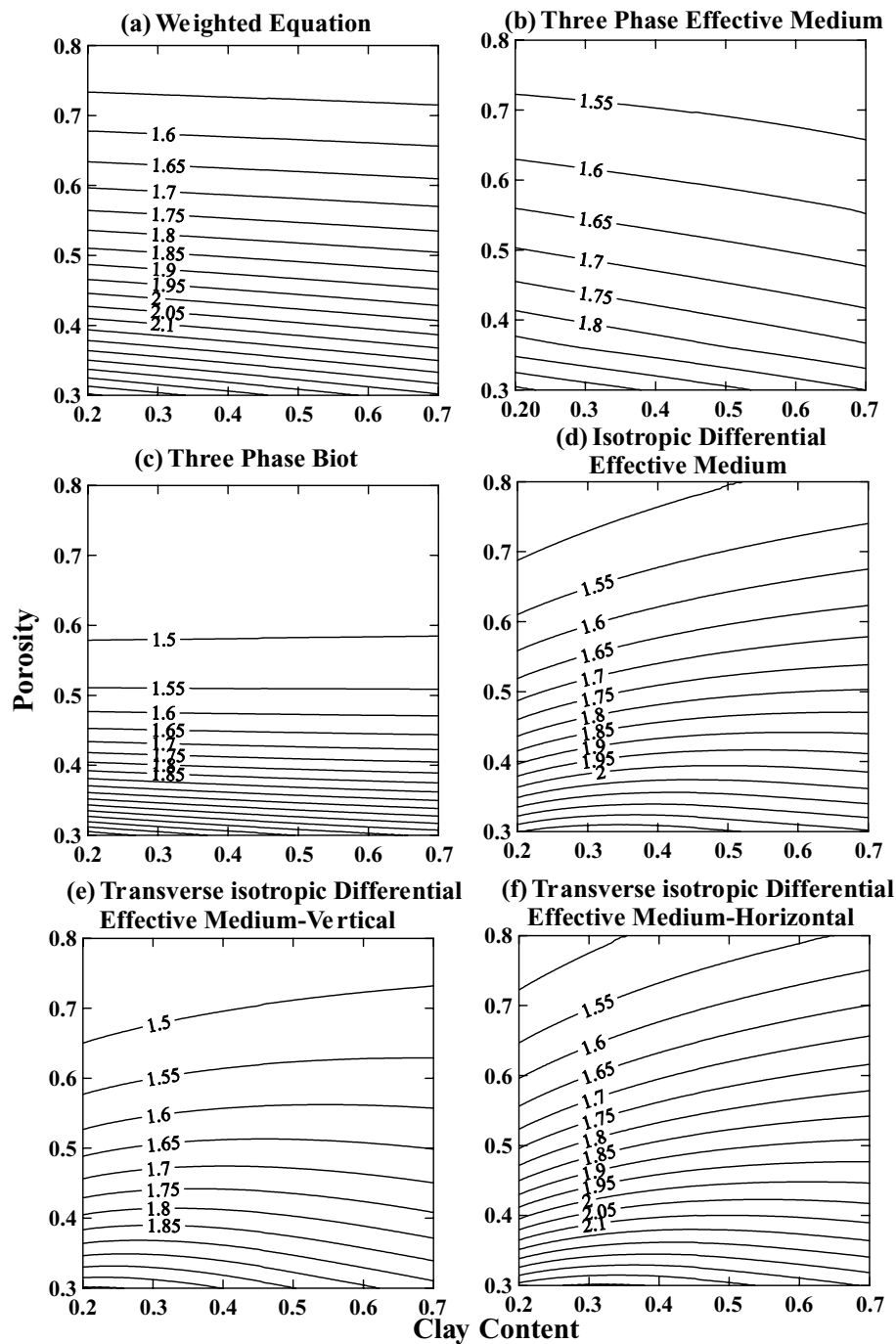


Figure 3. V_p as a function of porosity and clay content at 0 per cent hydrate saturation for different models: (a) WE, (b) TPBM, (c) TPB, (d) isotropic DEM, (e) vertical velocity for the transverse isotropic DEM model with an aspect ratio of 0.05, (f) horizontal velocity for the transverse isotropic DEM model.

The velocities predicted by different models for non-hydrate-bearing sediments are within the range of velocities observed *in situ* except for the WE model at low porosities and the TPB model at higher porosities, when anomalously low velocities are predicted. For example, the sediments from the non-hydrate-bearing zones of the Mallik 2L-38 well have V_p and V_s values of 2.0–2.2 km s⁻¹ and 0.5–0.8 km s⁻¹, respectively, for 30–40 per cent porosity and 30–40 per cent clay content (Guerin & Goldberg 2002), which do not match with those predicted by the WE model. For the clay-rich sediments of ODP Site 164 on Blake Ridge, the V_p and V_s values observed in the non-hydrate-bearing zones are 1.5–1.6 and 0.35–

0.4 km s⁻¹, respectively, with 60–70 per cent porosity and 60–70 per cent clay content (Guerin *et al.* 1999), which do not match with those predicted by the TPB model. The accuracy of these two methods (WE and TPB) could be improved by calibrating them more explicitly with data from these sites.

The four models predict similar variations of V_p with hydrate saturation (Fig. 5). For the WE model, V_p ranges between 4.0 and 1.6 km s⁻¹ for porosity varying between 80 and 30 per cent and hydrate saturation between 0 and 100 per cent of the pore space (Fig. 5a). For the TPBM model, V_p ranges between 4.0 and 1.8 km s⁻¹, while for the TPB model the range is 4.2–1.6 km s⁻¹ (Fig. 5c)

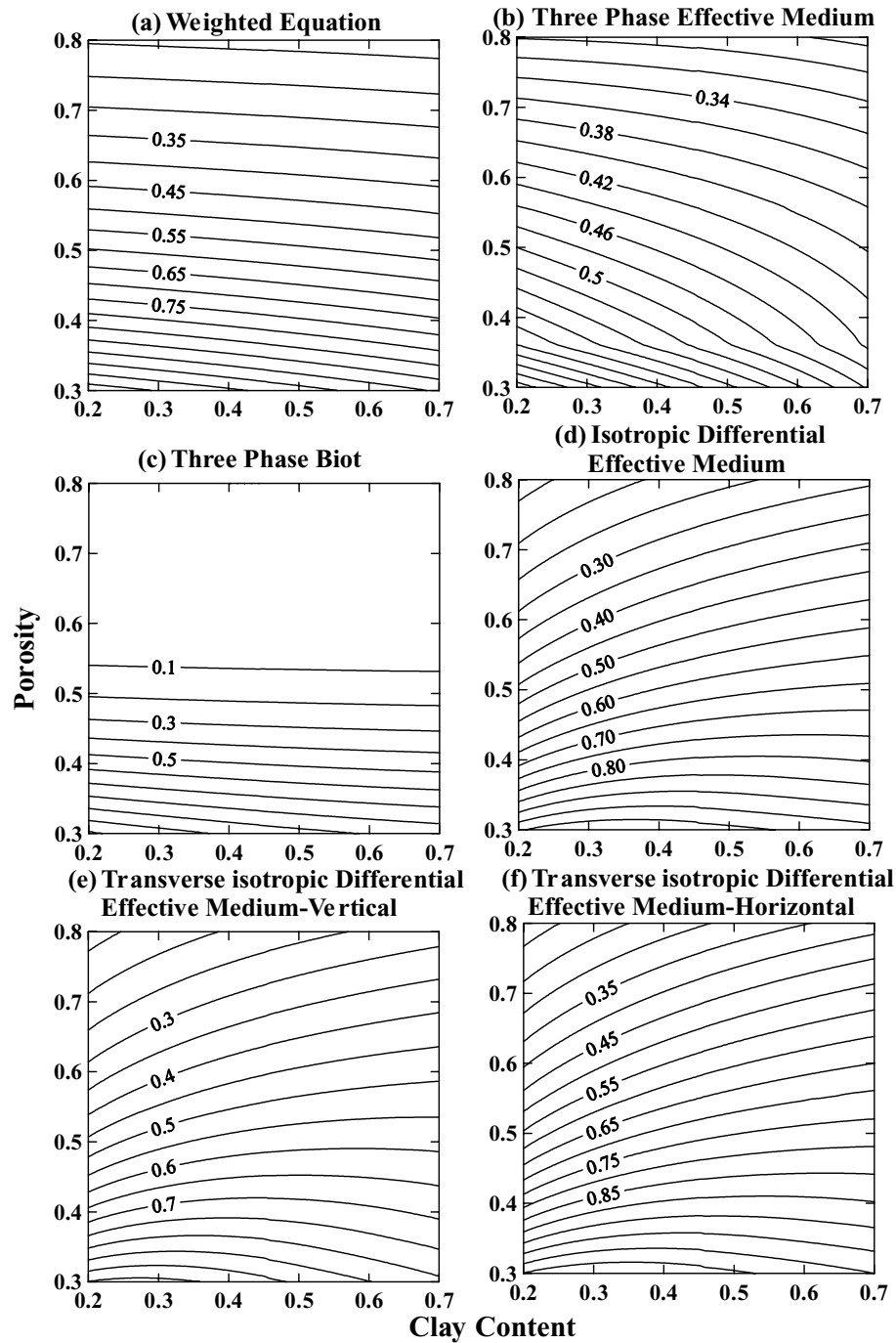


Figure 4. V_s as a function of porosity and clay content at 0 per cent hydrate saturation for different models: (a) WE, (b) TPBM, (c) TPB, (d) isotropic DEM, (e) vertical velocity for the transverse isotropic DEM model with an aspect ratio of 0.05, (f) horizontal velocity for the transverse isotropic DEM model.

and for the isotropic DEM model it is 3.8–1.8 km s⁻¹ (Fig. 5d). For the transverse isotropic DEM model, the vertical V_p varies between 3.8 and 1.8 km s⁻¹ (Fig. 5e). For the DEM cemented model, V_p varies between 3.6 and 1.8 km s⁻¹ (Fig. 5f). The major difference between using a clay–hydrate starting model and using a clay–water starting model in the DEM is that in the first case the velocities are higher at lower hydrate saturations (Fig. 5f). The TPB model predicts little variation of V_p with hydrate saturation below ~20 per cent (Fig. 5c).

The models predict similar patterns for S -wave velocities. The WE model predicts values of 0.4–2.4 km s⁻¹ for the range of porosi-

ties considered, with a sharp increase at higher hydrate saturations (Fig. 6a). The TPBM model predicts values of 0.4–2.2 km s⁻¹ (Fig. 6b). As for V_p , the TPB model predicts strong dependence on hydrate saturation only above ~20 per cent saturation, and V_s ranges between 2.6 and 0.2 km s⁻¹ (Fig. 6c). The isotropic DEM model predicts a similar pattern as for V_p , with V_s ranging between 2.2 and 0.4 km s⁻¹ (Fig. 6d). For the transverse isotropic DEM model the vertical velocity ranges between 2.0 and 0.3 km s⁻¹ (Fig. 6e). For the DEM cemented model, V_s ranges between 2.0 and 0.6 km s⁻¹ and velocities are higher at low hydrate saturations than for the DEM contact model (Figs 6d and f).

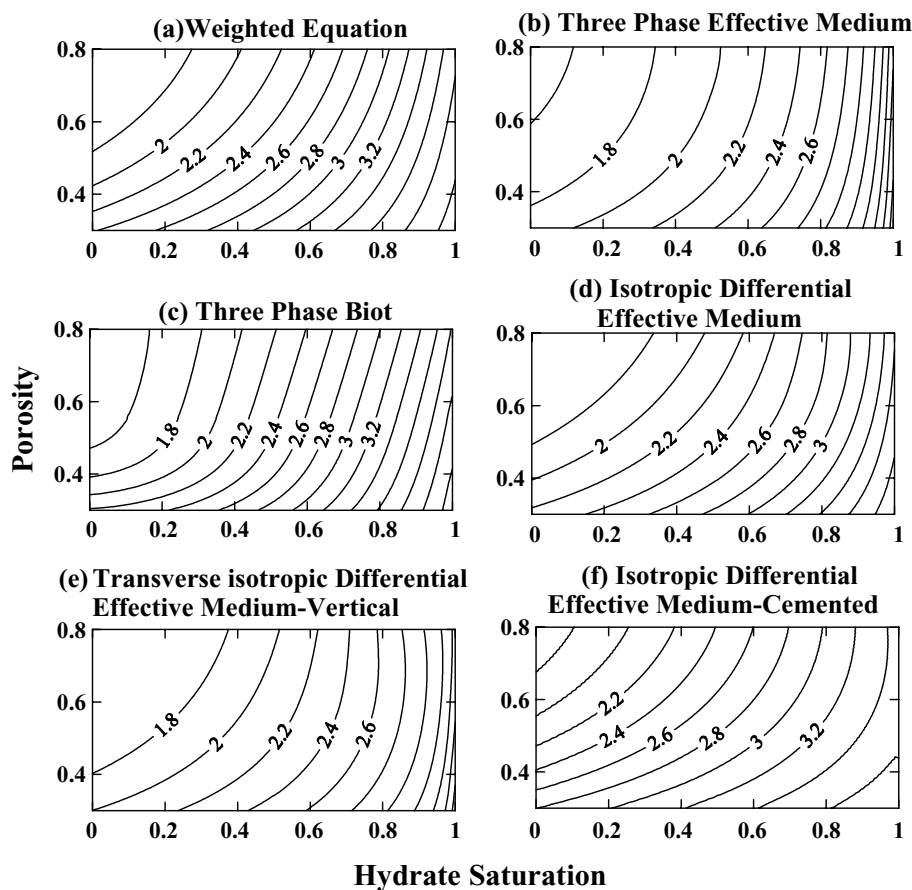


Figure 5. V_p as a function of porosity and hydrate saturation at 50 per cent clay content for different models: (a) WE, (b) TPBM, (c) TPB, (d) isotropic DEM model with clay–water starting model, (e) vertical velocity for transverse isotropic DEM model with clay–water starting model and an aspect ratio of 0.05, (f) isotropic DEM model with clay–hydrate starting model.

For all models the V_p/V_s ratios decrease with increasing hydrate saturation and porosity (Fig. 7). However, the magnitude of the change varies; for example, the DEM model with clay–water as the starting medium predicts a very small variation with hydrate saturation. The DEM cemented model predicts the lowest V_p/V_s ratios (Fig. 7f), implying low Poisson ratios comparable to that of a well-lithified rock (Fig. 7f).

From the above results we can conclude that all the models predict similar variations of V_p and V_s with hydrate saturation and clay content except for the DEM model, which predicts an increase in velocity with clay content. However, subtle differences between model predictions mean that for a given observed V_p and V_s , the predicted hydrate saturation will be different. In particular, the DEM cementation model, with clay–hydrate as starting medium, predicts a more rapid increase of velocity with hydrate as starting medium at low hydrate saturations.

4 APPLICATION TO REAL DATA

There are no published laboratory data sets of both V_p and V_s for real sediment samples containing known hydrate saturations though there are measurements made on artificial sediment samples containing hydrate (Kunerth *et al.* 2001; Berge *et al.* 1999) and measurements of V_p alone on natural sediment samples containing hydrates (Stoll *et al.* 1971; Stoll & Bryan 1979; Pearson *et al.* 1986; Winters *et al.* 2000). Therefore we use two field data sets to eval-

uate the effective-medium models on their ability to predict the correct velocities. The two data sets are borehole seismic log and VSP measurements, from the Mallik 2L–38 well, Mackenzie Delta, Canada (Collett *et al.* 1999; Katsube *et al.* 1999; Walia *et al.* 1999; Goldberg *et al.* 2000) and from Blake Ridge, ODP Sites 995 and 997 (Guerin, personal communication; Guerin *et al.* 1999; Wood & Ruppel 2000).

4.1 Mallik 2L–38 well, Mackenzie Delta, Canada

The Mallik 2L–38 well was drilled in a permafrost area with a permafrost thickness of 640 m in the Mackenzie Delta area of Canada (Collett *et al.* 1999; Katsube *et al.* 1999). NMR spectroscopy as well as Raman spectroscopy and gas to water ratios from a dissociation test showed that the hydrate in the well has properties similar to those of structure I hydrates (Uchida *et al.* 1999). An Archie's law interpretation of resistivity logs suggests that gas hydrate occupies an average of 47 per cent of the void space, increasing locally to 80 per cent (Fig. 8; Collett *et al.* 1999). Pore waters from the gas-hydrate-bearing samples had salinity values as low as 8 parts per trillion (ppt) compared with 34 ppt for non-gas-hydrate-bearing samples, suggesting that up to 80–90 per cent of the pore space in the gas-hydrate-bearing sediment might have been filled with gas hydrate (Cranston 1999). But the saturations predicted using chlorinity and those using resistivity and dissociation experiments differ widely from chlorinity-based predictions, being often lower (Guerin

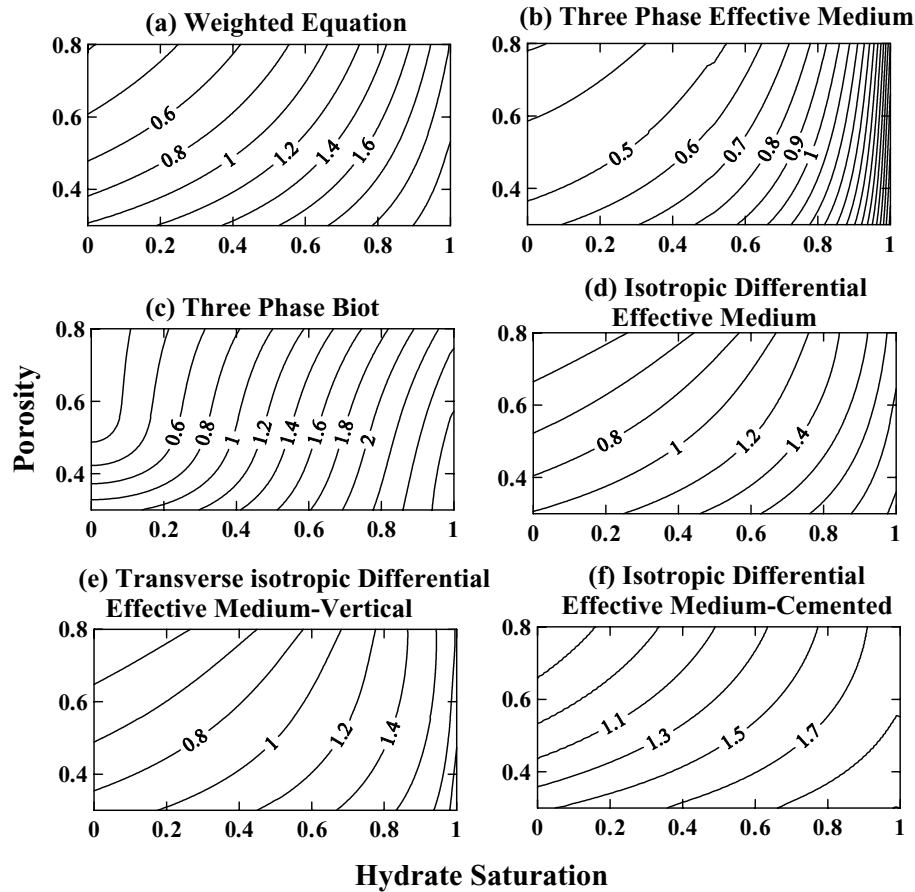


Figure 6. V_s as a function of porosity and hydrate saturation at 50 per cent clay content for different models: (a) WE, (b) TPME, (c) TPB, (d) isotropic DEM model with clay–water starting model, (e) vertical velocity for transverse isotropic DEM model with clay–water starting model and an aspect ratio of 0.05, (f) isotropic DEM model with clay–hydrate starting model.

& Goldberg 2002). Lee & Collett (1999) predicted around 80 per cent hydrate saturation using the WE model with a weighting factor of $W = 1.56$ and used $W = 1.44$ for another study on the same data set (Lee & Collett 2001).

Log and VSP results from the Mallik well are summarized in Fig. 8. The log measurements were made at 12 and 2.5 kHz for compressional and shear waves respectively (Guerin & Goldberg 2002). The VSP measurements were made at 100 and 30 Hz peak frequencies for compressional and shear waves respectively (Sakai 1999). Since the clay content is not known at all depths we used gamma-ray data to estimate it. The available clay content estimates from XRD analysis (Katsube *et al.* 1999) were averaged and the equivalent gamma-ray units calculated using the average mineralogy of clay (Katsube *et al.* 1999) and standard gamma-ray American Petroleum Institute (API) values for clay minerals (Rider 1996). Clay contents were then computed by scaling the above average by the ratio of the observed gamma-ray values to the value calculated above. Individual horizons of very high hydrate saturation coincide with levels of low clay content (Fig. 8). Thus hydrate seems to occupy preferentially the larger pores, though the total porosity varies little through the GHSZ. It can be observed that individual zones of high velocity for V_p and V_s coincide with increase of resistivity and low clay content, implying that both velocities increase simultaneously with hydrate saturation.

Hydrate saturations obtained through inversion of both log and VSP velocities along with those obtained from resistivity log are

given in Fig. 9. The estimates from resistivity data may be influenced by the variation of pore-water salinity. For example, salinities as low as 8 ppt are reported in hydrate-bearing zones compared with 34 ppt for non-hydrate-bearing zones of the Mallik well (Cranston 1999; Winters *et al.* 1999). Thus, low chloride concentrations which indicate formation of hydrate cause an increase in the electrical resistivity independent of that due to the hydrate itself (Collett & Ladd 2000). The quality of coupling of resistivity sensors with the formation also affects the measured resistivity (Collett & Ladd 2000). The estimate based on chloride anomalies depends strongly on the assumed baseline for no hydrate. Also there could be interference of drilling fluid with the pore water (Lu & McMechan 2002). Hence there is an uncertainty in the estimation based on resistivity and chloride methods amounting to as much as 5 per cent entirely due to pore-water freshening alone (Collett & Ladd 2000). The major uncertainty in the sonic velocity comes from the intrinsic problems with velocity measurements due to weak coupling of the sonic tool to the borehole wall. The uncertainty in V_s measurements can be as much as 10 per cent due to dispersion in larger hole diameters and slow formations while V_p measurements are comparatively robust (Harrison *et al.* 1990).

All the models give consistent results for both V_p and V_s from log and VSP measurements. The estimated saturation values range between 60 and 80 per cent. The hydrate saturation estimated from V_s data is lower than that from V_p data except when the WE method is used, but here the V_s is estimated from V_p . This observation indicates

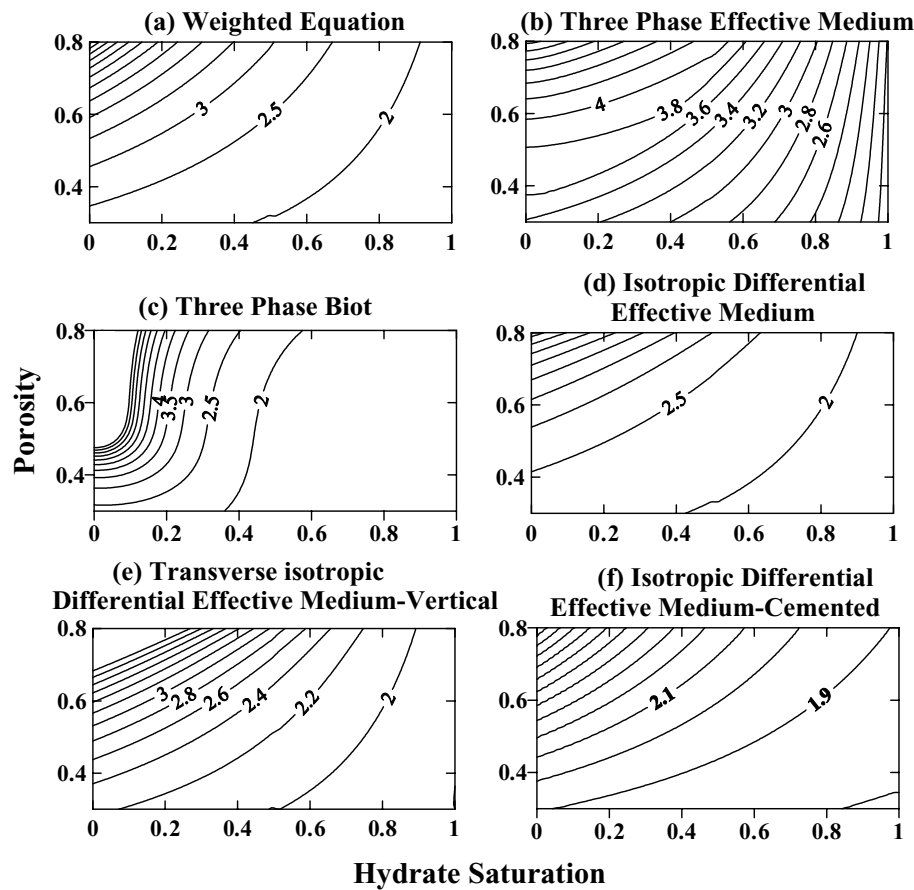


Figure 7. V_p/V_s ratios for hydrate-bearing sediments: (a) WE, (b) TPME, (c) TPB, (d) isotropic DEM model with clay–water starting model, (e) vertical velocity for the transverse isotropic DEM model with clay–water starting model and an aspect ratio of 0.05, (f) isotropic DEM model with clay–hydrate starting model.

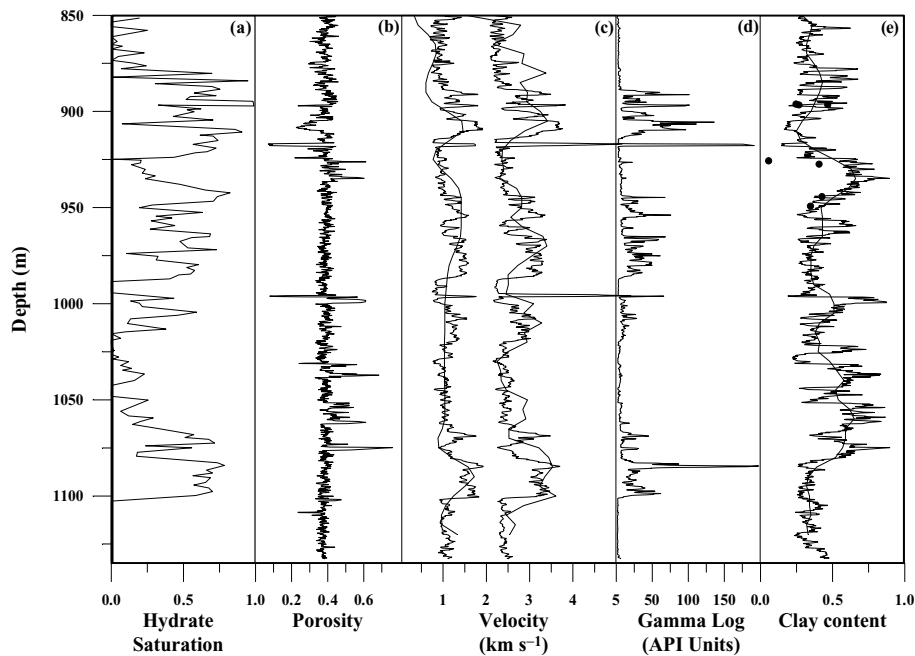


Figure 8. Bore hole geophysical data from the Mallik 2L–38 well, Mackenzie Delta, Canada: (a) hydrate saturation estimated from resistivity data (Collett *et al.* 1999), (b) porosity (Collett *et al.* 1999), (c) V_p and V_s data from acoustic log measurements (solid line) (Collett *et al.* 1999) and VSP data (dotted line) (Walia *et al.* 1999), (d) gamma-ray log (Collett *et al.* 1999), (e) clay content (percentage of solid volume) estimated using XRD (dots) (Katsube *et al.* 1999) and from gamma-ray log data. Notice the correlation of high hydrate saturation zones with low clay content zones.

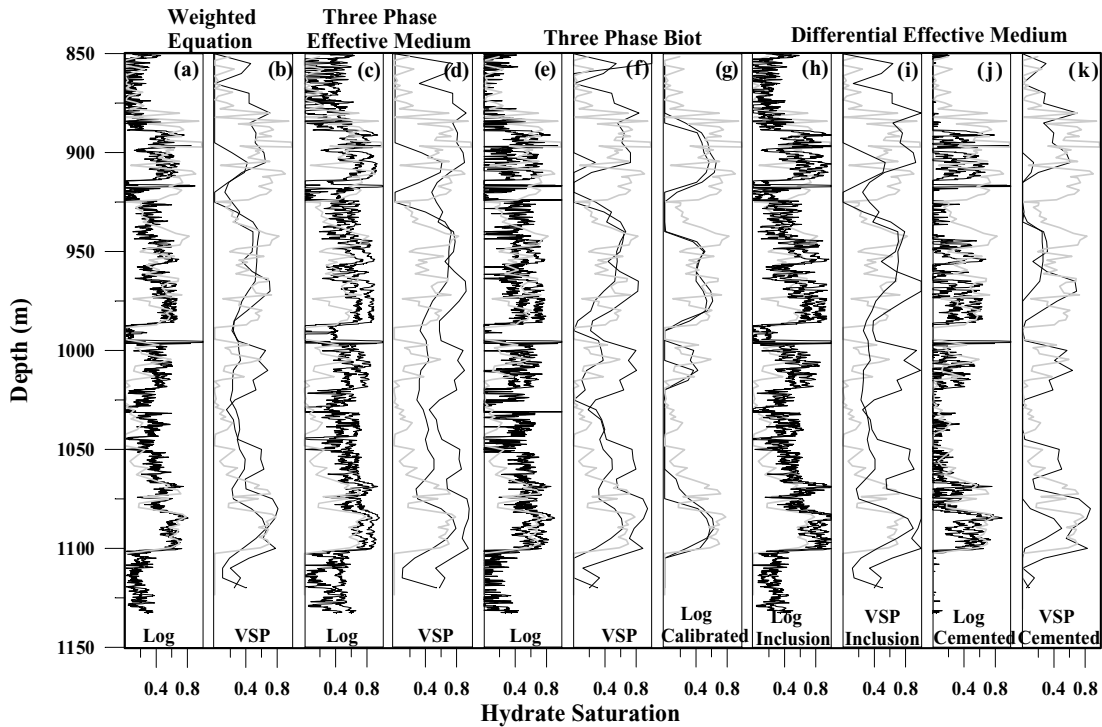


Figure 9. Hydrate saturation estimated using V_p (solid line) and V_s (dotted line) from both log and VSP data at the Mallik 2L–38 well, Mackenzie Delta, Canada. (a) From log data using the WE model. (b) From VSP data using the WE model. (c) From log data using the TPBM model. (d) From VSP data using the TPBM model. (e) From log data using the TPB model. (f) From VSP data using the TPB model. (g) From log data using the TPB model and the matrix properties calibrated from VSP (Walia *et al.* 1999). (h) From log data using the isotropic DEM model with clay–water as the starting medium. (i) From VSP data using the same model. (j) From log data using the isotropic DEM model with clay–hydrate as the starting medium. (k) From VSP data using the same model. The thick grey line marks hydrate saturation estimated from resistivity data.

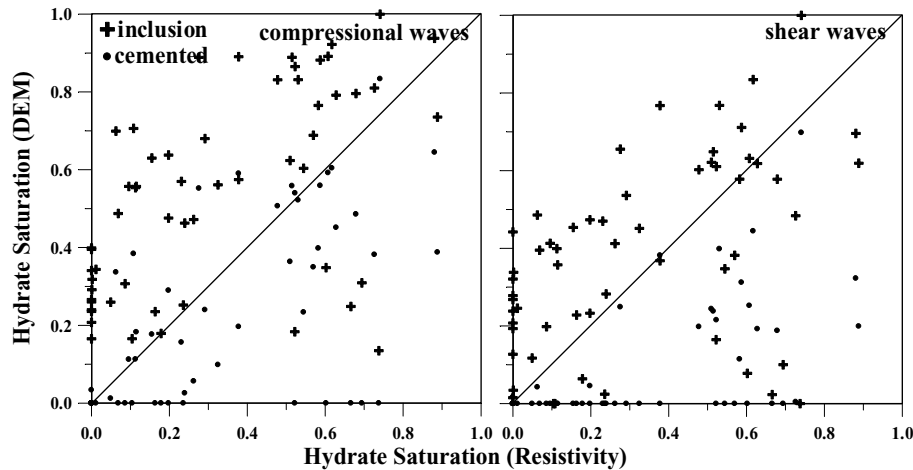


Figure 10. Comparison between hydrate saturations predicted using the two isotropic DEM models and log velocities as functions of saturation derived from resistivity data for the Mallik 2L–38 well (data smoothed and sampled at 5 m intervals). The solid line marks where two results are equal.

that the theories are predicting V_s values that are too high for a given hydrate content. We used $W = 1.0$ for the WE model since this model predicts lower velocities at lower porosities and any increase in W favours the Wood equation, thus further lowering the velocities with respect to *in situ* values. Although the estimated saturation values based on V_p and V_s match each other, only the WE, TPB and DEM with a clay–hydrate starting model (Fig. 9) match well the estimates from resistivity data. The TPBM models predict hydrate saturations that are systematically higher than those inferred from resistivity

data, with differences reaching 20 per cent at low hydrate saturations similar to those observed for the DEM model with clay–water as the starting medium. This difference may be due to the poor prediction of velocities of non-hydrated sediment by the TPBM model for this mineralogy. To compare predictions from calibrated and non-calibrated TPB models, we calculated the matrix properties by fitting the VSP data with a line connecting zones of no hydrate regions, and using Gassmann's equation. These estimates are only first-order estimates, since the formation changes from clay-rich zones outside

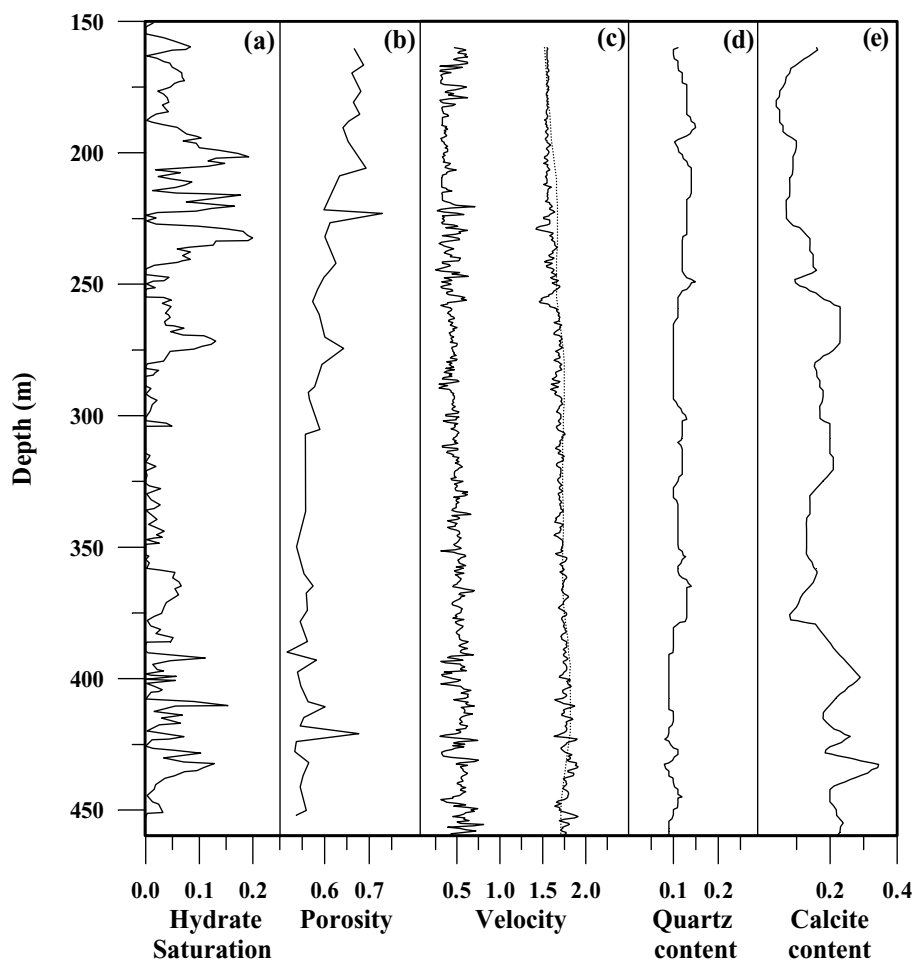


Figure 11. Bore hole geophysical data from ODP Site 995, Blake Ridge, Leg 164: (a) hydrate saturation estimated from resistivity data (Collett & Ladd 2000), (b) porosity (Guerin *et al.* 1999), (c) V_p and V_s data from acoustic log measurements (solid line) (Guerin *et al.* 1999) and VSP data (dotted line) (Wood & Ruppel 2000), (d) quartz content and (e) calcite content (per cent of solid volume) estimated using XRD (Collett & Wendlandt 2000).

the gas-hydrate zone to sand-rich zones inside. The VSP-calibrated log results using the TPB model (Fig. 9) give a well-defined picture of the hydrate and non-hydrate zones, though the predicted hydrate saturations are lower than those inferred from resistivity data. The hydrate saturation predicted by the DEM model with clay-hydrate as the starting medium matches better the resistivity-derived data, indicating that here hydrate forms a connected structure within the sediment frame (Figs 9 and 10).

4.2 Blake Ridge, ODP Sites 995 and 997

ODP Drilling Leg 164 in the Blake Ridge area on the US Atlantic margin produced both V_p and V_s logs (Guerin *et al.* 1999) (Figs 11 and 12). Blake Ridge sediments contain clay as a major constituent (Collett & Wendlandt 2000). Inferred hydrate saturation is low, ~2–11 per cent of the bulk volume (6–20 per cent pore volume), in the GHSZ of the Blake Ridge area (Holbrook *et al.* 1996; Paull *et al.* 1996; Guerin *et al.* 1999; Collett & Ladd 2000; Collett & Wendlandt 2000; Lee 2000; Tinivella & Lodolo 2000) (Figs 11 and 12). We used log (both V_p and V_s) and VSP (only V_p) data (Guerin, personal communication; Guerin *et al.* 1999; Wood & Ruppel 2000) and other measured parameters such as porosity (Lee 2000; Guerin *et al.* 1999) and quartz and calcite content (Collett & Wendlandt 2000) from ODP Sites 995 and 997, to estimate the hydrate satu-

ration. The log data were collected using 13 and 3 kHz sources for compressional and shear waves respectively (Guerin *et al.* 1999). The VSP data were acquired with a dominant frequency of 100 Hz (Wood & Ruppel 2000). One major difference observed in the Blake Ridge data is that unlike the Mallik data set, where both velocities increase simultaneously, the shear velocities are not showing a similar pattern to that of compressional wave velocities (Figs 11 and 12).

Estimated hydrate saturation values are shown in Figs 13–16. Only the DEM (clay-hydrate starting model), TPBM and WE models give hydrate saturation from V_p data that is comparable to that predicted from resistivity data (Figs 13 and 15). The resistivity-derived values may be overestimates here, since non-zero hydrate saturations are inferred in non-hydrate-bearing zones at shallow depths, and values are higher than those inferred from pore-water chlorinity data (Collett & Ladd 2000). The predicted hydrate saturation from V_s is very low or zero for the case of DEM and TPBM models, while WE and TPB models predict higher hydrate saturations than those predicted from V_p . The DEM (Fig. 13g) model with hydrate as inclusions predicts consistently higher hydrate saturations than those estimated from resistivity data and other studies. The degree of anisotropy used in the DEM model broadly matches observations (Pecher *et al.* 2003). The TPB model predicts higher hydrate saturations than the other models (Figs 13i and j and 15i

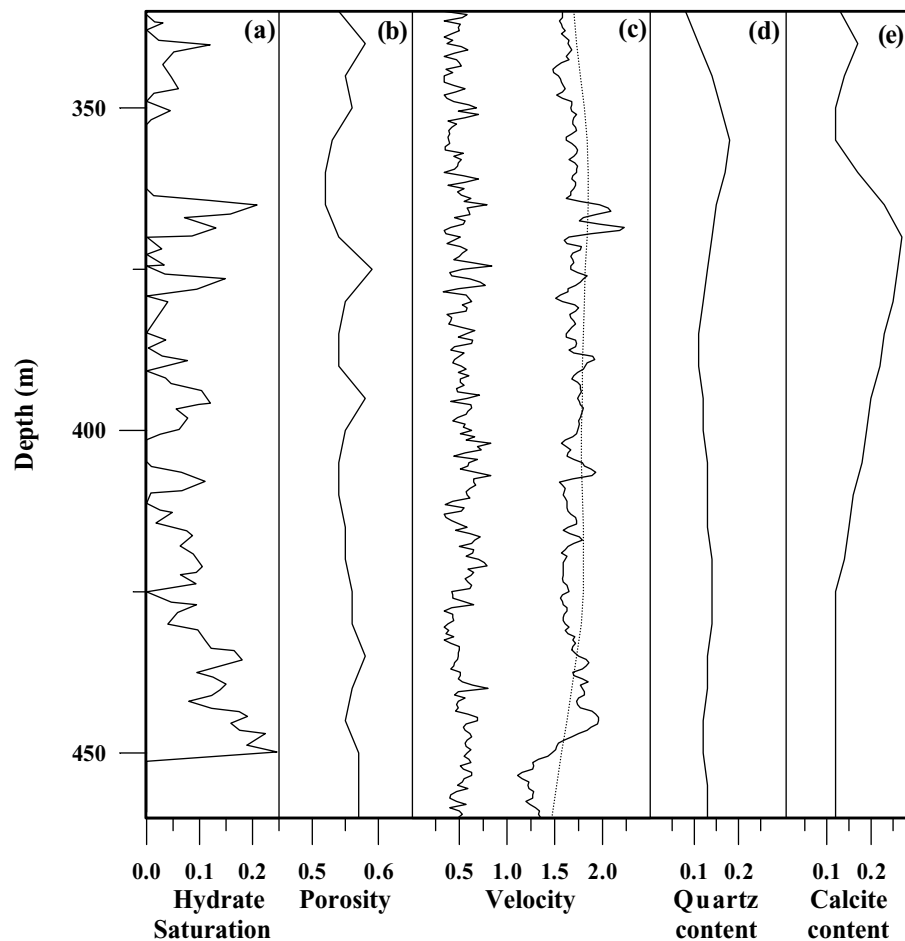


Figure 12. Bore hole geophysical data from ODP Site 997, Blake Ridge, Leg 164: (a) hydrate saturation estimated from resistivity data (Collett & Ladd 2000), (b) porosity (Lee 2000), (c) V_p and V_s data from acoustic log measurements (solid line) (Guerin, personal communication) and VSP data (dotted line) (Wood & Ruppel 2000), (d) quartz content and (e) calcite content (per cent of solid volume) estimated using XRD (Collett & Wendlandt 2000).

and j). As shown above, velocities predicted by the TPB model vary only very little with increase in hydrate saturation at low hydrate saturations, making the predictions unreliable at these saturations. In fact, as pointed out earlier, shear velocity perturbations show no correlation with perturbations of compressional wave velocity. However, given the low hydrate saturations, the expected perturbations in shear wave velocity due to any cementing effect of the hydrate are small. Therefore such perturbations may be difficult to decouple from those due to lithology, or to distinguish from variations due to the poor coupling of the shear wave tool in such high-porosity and low-velocity sediments.

5 DISCUSSION

Model results for non-hydrate-bearing sediments are generally comparable to the observed values of V_p and V_s except in the case of the WE, which predicts lower velocities at low porosities. This mismatch for the WE model may be due to an over-influence of Wood's equation on the final results at low porosities when actually the time-average equation could have been sufficient alone. The flat response of the TPB model at higher porosities (>60 per cent) is also unsatisfactory. The TPB model is designed to use calibrated data for the sediment properties; in situations where no physical measurements of sediments are available the high-porosity results should be

treated with caution. The DEM model predicts an increase in velocity with clay content, which is unrealistic at least at low porosities, where observations suggest the opposite. This behaviour is due to the dominant effect of the initial self-consistent approximation.

Our results contradict those of Ecker *et al.* (1998), who modelled the amplitude versus offset (AVO) response of a BSR at Blake Ridge. They looked at the two possible end-member scenarios; one in which hydrate is cementing the medium (TPEM models 1 and 2, Fig. 2) and the other in which hydrate lies away from the grains and does not affect the S -wave velocities (TPEM model 3, Fig. 2). Comparing the AVO observations with the model results, they concluded that the model in which hydrate lies away from the grains can match the observations, whether or not gas is present beneath the BSR. However, observations from the Mallik 2L-38 well (Collett *et al.* 1999) have shown that the S -wave velocity does increase with hydrate saturation. Other authors have concluded that the AVO response of BSRs is dominated by the effect of gas beneath the BSR (e.g. Minshull *et al.* 1994; Andreassen *et al.* 1995, 1997; Tinivella & Accaino 2000) and by the thickness of the gas zone (e.g. Xu & Chopra 2003). The major effect of the gas zone means that inferences about the presence or absence of hydrate cementation from AVO anomalies may be unreliable.

The various effective-medium models predict quite different hydrate saturations when applied to field data sets. The WE and TPB

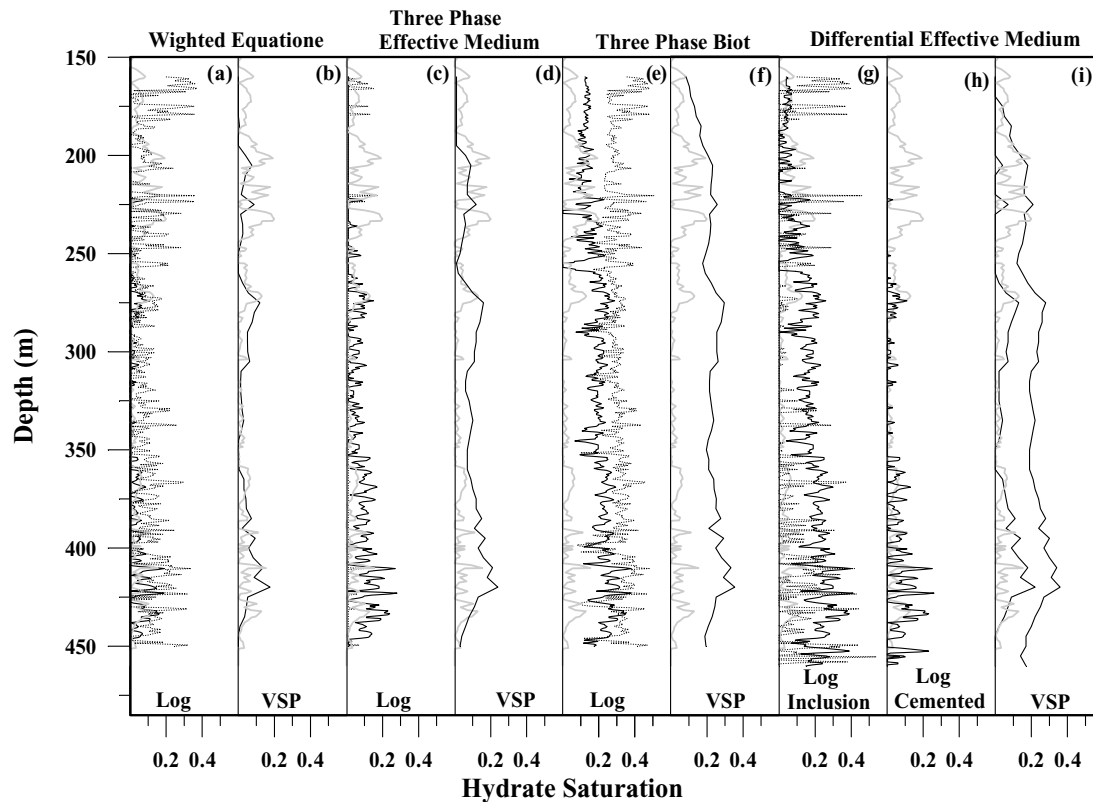


Figure 13. Hydrate saturation estimated using V_p (solid line) and V_s (dotted line) data from both log and VSP data at ODP Site 995, Leg 164, Blake Ridge. (a) From log data using the WE model. (b) From VSP data using the WE model. (c) From log data using the TPBM model. (d) From VSP data using the TPBM model. (e) From log data using the TPB model, (f) From VSP data using the TPB model. (g) From log data using vertical velocities from the transverse isotropic DEM model with clay–water as the starting medium. (h) From log data using vertical velocities from the transverse isotropic DEM model with clay–hydrate as the starting medium. (i) From VSP data using vertical velocities from the transverse isotropic DEM model and vertical velocities from the transverse isotropic DEM model (lower saturation) with clay–hydrate as starting medium. The thick grey line marks hydrate saturation estimated from resistivity data.

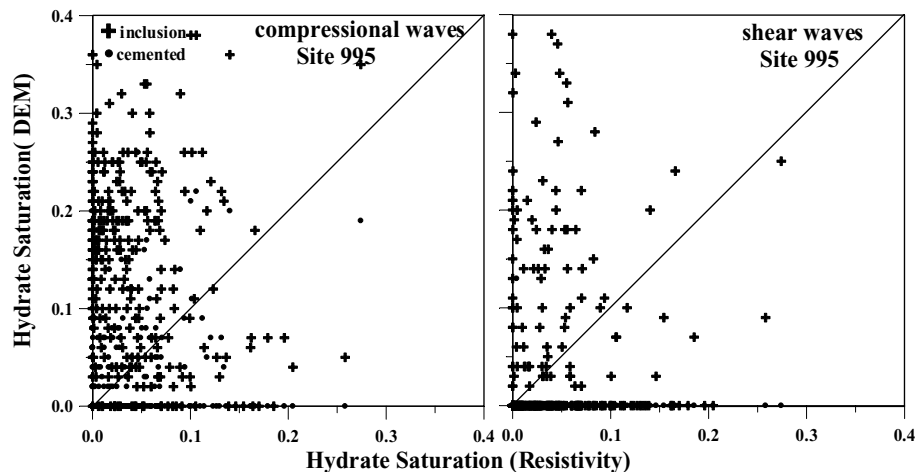


Figure 14. Comparison between hydrate saturations predicted using the two transversely isotropic DEM models and log velocities as functions of saturation derived from resistivity data for site 995 (data smoothed and sampled at 2.5 m intervals). The solid line marks where two results are equal.

models clearly need good calibration of the sediment properties. In the case of the WE model, a value of $W = 1.44$ (Lee & Collett 2001) will result in even lower predicted hydrate saturations, which are already too low for $W = 1$. The TPB model gives an improved result, when calibrated using VSP data as in the case of Mallik data set, but predicted saturations remain lower than resistivity-derived values. The TPBM model requires a further modification to predict

non-hydrate-bearing sediment properties as observed in the case of the Mallik data set where it predicts hydrate saturations even in hydrate-free zones. Both at Mallik and Blake Ridge, the DEM model with clay–hydrate as the starting medium predicts hydrate contents that are slightly lower than those inferred from resistivity data, and generally consistent with those inferred from chlorinity and headspace methane data.

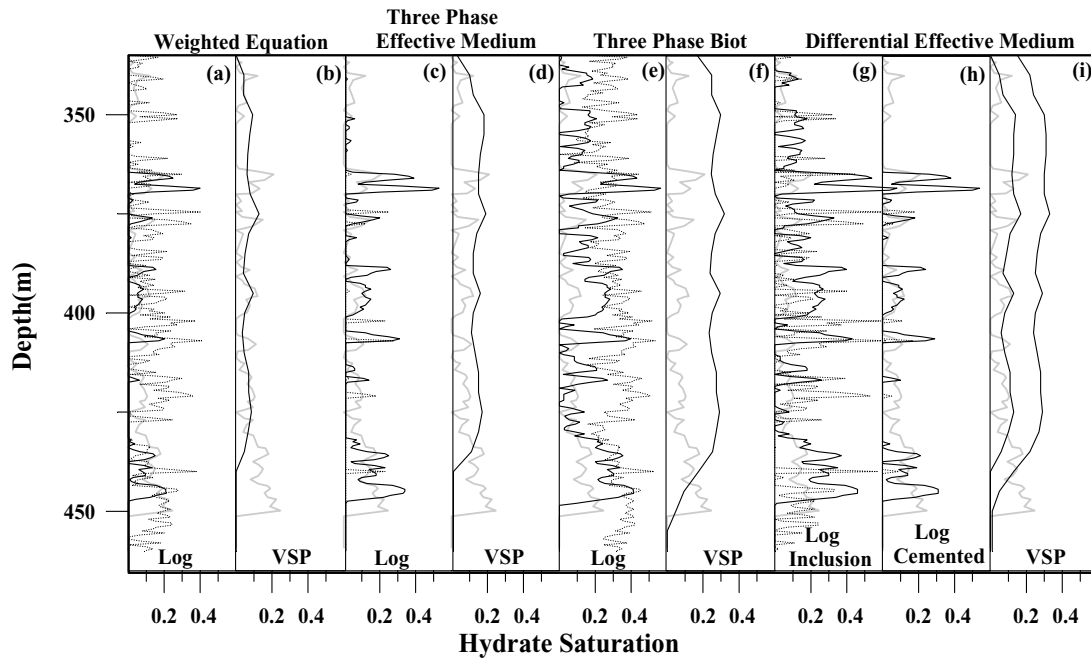


Figure 15. Hydrate saturation estimated using V_p (solid line) and V_s (dotted line) data from both log and VSP data at ODP Site 997, Leg 164, Blake Ridge. (a) From log data using the WE model. (b) From VSP data using the WE model. (c) From log data using the TPME model. (d) From VSP data using the TPME model. (e) From log data using the TPB model. (f) From VSP data using the TPB model. (g) From log data using vertical velocities from the transverse isotropic DEM model with clay–water as the starting medium. (h) From log data using vertical velocities from the transverse isotropic DEM model with clay–hydrate as the starting medium. (i) From VSP data using vertical velocities from the transverse isotropic DEM model and vertical velocities from the transverse isotropic DEM model (lower saturation) with clay–hydrate as the starting medium.

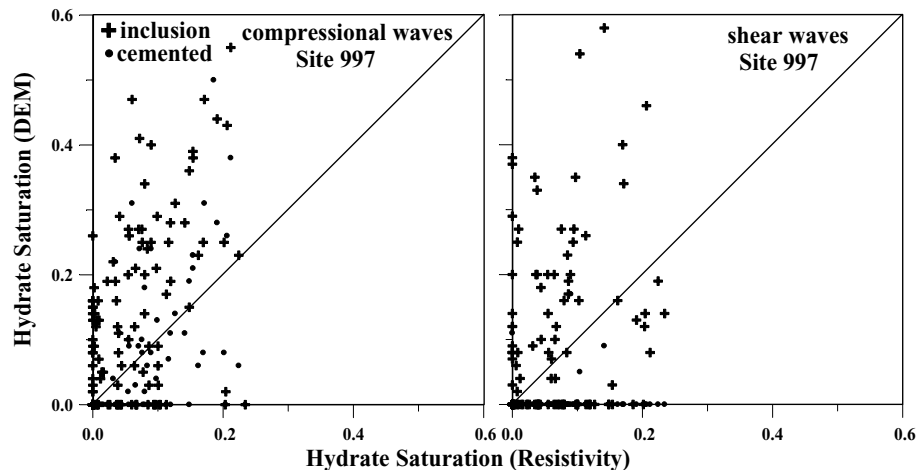


Figure 16. Comparison between hydrate saturations predicted using the two transverse isotropic DEM models and log velocities as functions of saturation derived from resistivity data for Site 997 (data smoothed and sampled at 2.5 m intervals). The solid line marks where the two results are equal.

6 CONCLUSIONS

From our analysis of a variety of effective-medium models, we conclude that:

(1) The four models investigated generally predict a similar range of V_p and V_s for hydrate-free saturated sediment samples, though details of their variation with porosity and clay content are different. In particular, the DEM model predicts the opposite variation with clay content than do the other models. Predicted velocities for hydrate-bearing saturated sediments also vary little, but the pattern of velocity variation with hydrate saturation differs between models. The TPB model exhibits only a very small increase in velocities with

hydrate saturation below 20 per cent saturation. The DEM model with a clay–hydrate starting medium predicts higher velocities at lower hydrate saturations than those predicted by other models.

(2) The DEM, TPB and WE models match hydrate saturations predicted from resistivity data from the Mallik 2L–38 well. The TPME model predicts hydrate saturations up to 20 per cent higher. The DEM model requires a clay–hydrate composite as the starting model to match the hydrate content inferred from resistivity data.

(3) For the clay-rich sediments of ODP Sites 995 and 997, Blake Ridge, the DEM, TPME and WE models predict comparable hydrate saturations of 10–20 per cent (~ 6 –12 per cent bulk volume) from V_p data. Since at low saturation hydrate may have little influence

on V_s , all the models except for WE and TPB predict zero hydrate saturation from V_s . Since the V_s predicted by the TPB model shows little dependence on hydrate saturation at low values, a small change in V_s leads to a very high inferred hydrate saturation.

(4) The success of the DEM model with a clay–hydrate starting model suggests that hydrates form a connected phase affecting the rock framework, rather than disconnected inclusions.

ACKNOWLEDGMENTS

We thank Dr Giles Guerin for providing sonic V_p and V_s data from ODP Leg 164, Sites 995 and 997, Blake Ridge. This work was funded by the European Union through the HYDRATECH project (EVK3-2000-22060). We thank Ingo Pecher, Ingo Grevenmeyer and Warren Wood for their constructive comments which helped us to improve this manuscript.

REFERENCES

- Andreassen, K., Hart, P.E. & Grantz, A., 1995. Seismic studies of a bottom simulating reflection related to gas hydrate beneath the continental margin of the Beaufort Sea, *J. geophys. Res.*, **100**, 12 659–12 673.
- Andreassen, K., Hart, P.E. & MacKay, M., 1997. Amplitude versus offset modelling of the bottom simulating reflection associated with submarine gas hydrates, *Mar. Geol.*, **137**, 25–40.
- Bennett, R.H., Bryant, W.R. & Hulbert, M.H., 1991. *Microstructure of Fine-Grained Sediments: From Mud to Shale* Springer, New York.
- Berge, L.N., Jacobsen, K.A. & Solstad, A., 1999. Measured acoustic wave velocities of R11 (CCl₃F) hydrate samples with and without sand as a function of hydrate concentration, *J. geophys. Res.*, **104**, 15 415–15 424.
- Blangy, J.P., Strandesen, S., Moos, D. & Nur, A., 1993. Ultrasonic velocities in sands—revised, *Geophysics*, **58**, 344–356.
- Bonilla, L.L. & Keller, J.B., 1985. Acoustic elastic effect and wave propagation in heterogeneous weakly anisotropic materials, *J. Mech. Phys. Solids*, **33**, 241–261.
- Brooks, J., Cox, H., Bryant, W., Kennicutt, M. II, Mann, R. & McDonald, T., 1986. Association of gas hydrates and oil seepage in the Gulf of Mexico., *Org. Geochem.*, **10**, 221–234.
- Carcione, J.M. & Tinivella, U., 2000. Bottom-simulating reflectors: seismic velocities and AVO effects, *Geophysics*, **65**(1), 54–67.
- Carmichael, R.S., 1982. *Practical Handbook of Physical Properties of Rocks*, Vol. II, CRC Press, Boca Raton, FL.
- Chand, S. & Minshull, T.A., 2003. Seismic constraints on the effects of gas hydrate on sediment physical properties and fluid flow: a review, *Geofluids*, **3**, 1–15.
- Collett, T.S. & Ladd, J., 2000. Detection of gas hydrate with downhole logs and assessment of gas hydrate concentrations (saturation) and gas volumes on the Blake Ridge with electrical resistivity log data, in *Proceedings of the Ocean Drilling Program, Scientific Results 164*, pp. 179–191, eds Paull, C.K., Matsumoto, R., Wallace, P.J. & Dillon, W.P., Texas A&M University, College Station, Texas, Ocean Drilling Program.
- Collett, T.S. & Wendlandt, R.F., 2000. Formation evaluation of gas hydrate-bearing marine sediments on the Blake Ridge with downhole geochemical log measurements, in *Proceedings of the Ocean Drilling Program, Scientific Results 164*, pp. 199–215, eds Paull, C.K., Matsumoto, R., Wallace, P.J. & Dillon, W.P., Texas A&M University, College Station, Texas, Ocean Drilling Program.
- Collett, T.S., Lewis, R.E., Dallimore, S.R., Lee, M.W., Mroz, T.H. & Uchida, T., 1999. Detailed evaluation of gas hydrate reservoir properties using JAPEx/JNOC/GSC Mallik 2L-38 gas hydrate research well downhole well-log displays, in *Scientific Results From JAPEx/JNOC/GSC Mallik 2L-38 Gas Hydrate Research Well, Mackenzie Delta, Northwest Territories, Canada*, Geological Survey of Canada Bulletin 544, pp. 295–312, eds Dallimore, S.R., Uchida, T. & Collett, T.S., Geological Survey of Canada, Ottawa, Canada.
- Cranston, R.E., 1999. Pore-water geochemistry, JAPEx/JNOC/GSC Mallik 2L-38 gas hydrate research well, in *Scientific Results From JAPEx/JNOC/GSC Mallik 2L-38 Gas Hydrate Research Well, Mackenzie Delta, Northwest Territories, Canada*, Geological Survey of Canada Bulletin 544, pp. 165–175, eds Dallimore, S.R., Uchida, T. & Collett, T.S. Geological Survey of Canada, Ottawa, Canada.
- Davidson, D.W., Garg, S.K., Gough, S.R., Handa, Y.P., Ratcliffe, C.I., Ripmester, J.A., Tse, J.S. & Lawson, W.F., 1986. Laboratory analysis of a naturally occurring gas hydrate from sediment of the Gulf of Mexico, *Cosmochim. Acta*, **50**, 619–623.
- Dvorkin, J. & Nur, A., 1996. Elasticity of high-porosity sandstones: theory for two North Sea data sets, *Geophysics*, **61**, 1363–1378.
- Dvorkin, J., Mavko, G. & Nur, A., 1991. The effect of cementation on the elastic properties of granular material, *Mech. Mater.*, **12**, 207–217.
- Dvorkin, J., Nur, A. & Yin, H., 1994. Effective properties of cemented granular material, *Mech. Mater.*, **18**, 351–366.
- Eastwood, R.L. & Castagna, J.P., 1983. Basis for interpretation of V_s/V_p ratios in complex lithologies, *Proceedings of 24th SPWLA Annual Logging Symposium*, paper G. Reprinted in *Geophysics II, Tools for Seismic Interpretation, Treatise of Petroleum Geology*, American Association of Petroleum Geologists.
- Ecker, C., Dvorkin, J. & Nur, A., 1998. Sediments with gas hydrates: internal structure from seismic AVO, *Geophysics*, **63**, 1659–1669.
- Ecker, C., Dvorkin, J. & Nur, A., 2000. Estimating the amount of gas hydrate and free gas from marine seismic data, *Geophysics*, **65**(2), 565–573.
- Gassmann, F., 1951. Über die elastizität poröser medien, *Vierteljahr. Naturforsch. Gesell. Zurich*, **96**, 1–23.
- Gei, D. & Carcione, J.M., 2003. Acoustic properties of sediments saturated with gas hydrate, free gas and water, *Geophys. Prospect.*, **51**, 141–157.
- Goldberg, D.S., Collett, T.S. & Hyndman, R.D., 2000. Ground truth: in-situ properties of hydrate, in *Natural Gas Hydrate in Oceanic and Permafrost Environments*, pp. 295–310, ed. Max, M.D., Kluwer Academic, Dordrecht.
- Goldberg, I. & Gurevich, B., 1998. A semi-empirical velocity-porosity-clay model for petrophysical interpretation of P- and S-velocities, *Geophys. Prospect.*, **46**, 271–285.
- Guerin, G. & Goldberg, D., 2002. Sonic waveform attenuation in gas hydrate-bearing sediments from the Mallik 2L-38 research well, Mackenzie Delta, Canada, *J. geophys. Res.*, **107**, doi:10.1029/2001JB000556.
- Guerin, G., Goldberg, D. & Meltser, A., 1999. Characterization of *in situ* elastic properties of gas hydrate-bearing sediments on the Blake Ridge, *J. geophys. Res.*, **104**, 17 781–17 795.
- Harrisson, A.R., Randall, C.J., Aron, J.B., Morris, C.F., Wignall, A.H., Dworak, R.A., Rutledge, L.L. & Perkins, J.L., 1990. Acquisition and analysis of sonic waveforms from a borehole monopole and dipole source for the determination of compressional and shear speeds and their relation to rock mechanical properties and surface seismic data, *65th Annual Technical Conference and Exhibition*, pp. 267–282, SPE 20557, Society of Petroleum Engineers, New Orleans, LA.
- Helgerud, M.B., Dvorkin, J., Nur, A., Sakai, A. & Collett, T.S., 1999. Elastic-wave velocity in marine sediments with gas hydrates: effective medium modelling, *Geophys. Res. Lett.*, **26**, 2021–2024.
- Hill, R., 1952. The elastic behaviour of a crystalline aggregate, *Proc. Phys. Soc.*, **A65**, 349–354.
- Holbrook, W.S., Hoskins, H., Wood, W.T., Stephen, R.A., Lizarralde, D., 164. Science Party, 1996. Methane hydrate and free gas on the Blake ridge from vertical seismic profiling, *Science*, **273**, 1840–1843.
- Hornby, B.E., Schwartz, L.M. & Hudson, J.A., 1994. Anisotropic effective-medium modelling of the elastic properties of shales, *Geophysics*, **59**, 1570–1581.
- Hudson, J.A., 1991. Overall properties of heterogeneous material, *Geophys. J. Int.*, **107**, 505–511.
- Jakobsen, M., Hudson, J.A., Minshull, T.A. & Singh, S.C., 2000. Elastic properties of hydrate-bearing sediments using effective-medium theory, *J. geophys. Res.*, **105**, 561–577.
- Kastner, M., Kvenvolden, K.A. & Lorenson, T.D., 1998. Chemistry, isotopic composition and origin of a methane-hydrogen sulfide hydrate at the Cascadia subduction zone, *Earth planet. Sci. Lett.*, **156**, 173–183.

- Katsube, T.J., Dallimore, S.R., Uchida, T., Jenner, K.A., Collett, T.S. & Connell, S., 1999. Petrophysical environment of sediments hosting gas hydrate, JAPEx/JNOC/GSC Mallik 2L-38 gas hydrate research well, in *Scientific Results From JAPEx/JNOC/GSC Mallik 2L-38 Gas Hydrate Research Well, Mackenzie Delta, Northwest Territories, Canada*, Geological Survey of Canada Bulletin 544, pp. 109–124, eds Dallimore, S.R., Uchida, T. & Collett, T.S., Geological Survey of Canada, Ottawa, Canada.
- Krief, M., Garat, J., Stellingwerff, J. & Ventre, J., 1990. A petrophysical interpretation using the velocities of P and S waves (full waveform sonic), *Log Analyst*, **31**, 355–369.
- Kunerth, D.C., Weinberg, D.M., Rector, J.W. III, Scott, C.L. & Johnson, J.T., 2001. Acoustic laboratory measurements during the formation of a THF-hydrate in unconsolidated porous media, *J. Seismic Exploration*, **9**, 337–354.
- Kvenvolden, K.A., 1998. A primer on geological occurrence of gas hydrate, in *Gas Hydrates: Relevance to World Margin Stability and Climate Change*, Geological Society of London Special Publication 137, pp. 9–30, eds Henriot, J.P. & Mienert, J., Geological Society of London, London.
- Kvenvolden, K.A., 2000. Natural gas hydrate: introduction and history of discovery, in *Coastal Systems and Continental Margins, Natural Gas Hydrate in Oceanic and Permafrost Environments*, pp. 9–16, ed. Max, M.D., Kluwer Academic Press, Dordrecht.
- Leclaire, Ph., Cohen-Tenoudji, F. & Aguirre-Puente, J., 1994. Extension of Biot's theory of wave propagation to frozen porous media, *J. acoust. Soc. Am.*, **96**, 3753–3768.
- Lee, M.W., 2000. Gas hydrates amount estimated from acoustic logs at the Blake Ridge, Sites 994, 995, and 997, in *Proceedings of the Ocean Drilling Program, Scientific Results 164*, pp. 193–198, eds Paull, C.K., Matsumoto, R., Wallace, P.J. & Dillon, W.P., Texas A&M University, College Station, Texas, Ocean Drilling Program.
- Lee, M.W., 2002. Biot–Gassmann theory for velocities of gas hydrate-bearing sediments, *Geophysics*, **67**, 1711–1719.
- Lee, M.W. & Collett, T.S., 1999. Amount of gas hydrate estimated from compressional and shear wave velocities at the JAPEx/JNOC/GSC Mallik 2L-38 gas hydrate research well, in *Scientific Results From JAPEx/JNOC/GSC Mallik 2L-38 Gas Hydrate Research Well, Mackenzie Delta, Northwest Territories, Canada*, Geological Survey of Canada Bulletin 544, pp. 313–322, eds Dallimore, S.R., Uchida, T. & Collett, T.S., Geological Survey of Canada, Ottawa, Canada.
- Lee, M.W. & Collett, T.S., 2001. Comparison of elastic velocity models for gas-hydrate-bearing sediments, in *Natural Gas Hydrates: Occurrence, Distribution and Detection*, American Geophysical Union Geophysical Monograph 124, pp. 179–188, eds Paull, C.K. & Dillon, W.P., American Geophysical Union, Washington, DC.
- Lee, M.W., Hutchinson, D.R., Collett, T.S. & Dillon, W.P., 1996. Seismic velocities for hydrate-bearing sediments using weighted equation, *J. geophys. Res.*, **101**, 20 347–20 358.
- Lu, S. & McMechan, G.A., 2002. Estimation of gas hydrate and free gas saturation, concentration, and distribution from seismic data, *Geophysics*, **67**, 582–593.
- Mackay, M.E., Jarrard, R.D., Westbrook, G.K., Hyndman, R.D., 146. 1994. Origin of bottom-simulating reflectors: geophysical evidence from the Cascadia accretionary prism, *Geology*, **22**, 459–462.
- Malone, R.D., 1985. Gas hydrates topical report, *Report DOE/METC/SP 218*, US Department of Energy, Washington, DC.
- Marion, D., Nur, A., Yin, H. & Han, D., 1992. Compressional velocity and porosity in sand-clay mixtures, *Geophysics*, **57**, 554–563.
- Mavko, G.T., Mukherji, T. & Dvorkin, J., 1998. *The Rock Physics Handbook—Tools for Seismic Analysis in Porous Media*, Cambridge University Press, New York.
- Mindlin, R.D., 1949. Compliance of elastic bodies in contact, *J. Appl. Mech.*, **16**, 259–268.
- Minshull, T.A., Singh, S.C. & Westbrook, G.K., 1994. Seismic velocity structure at a gas hydrate reflector, offshore western Columbia, from full waveform inversion, *J. geophys. Res.*, **99**, 4715–4734.
- Murphy, W.F.I., 1982. Effects of microstructure and pore fluids on the acoustic properties of granular sedimentary materials, *PhD Thesis*, Stanford University.
- Nishizawa, O., 1982. Seismic velocity anisotropy in a medium containing oriented cracks: transversely isotropic case, *J. Phys. Earth*, **30**, 331–347.
- Nur, A., Mavko, G., Dvorkin, J. & Galmudi, D., 1998. Critical porosity: a key to relating physical properties to porosity in rocks, *Leading Edge*, **17**, 357–362.
- Paull, C.K., Matsumoto, R., Wallace, P.J. & Shipboard Scientific Party., 1996. *Proceedings of the Ocean Drilling Program, Initial Reports 176*, Ocean Drilling Program, College Station, TX.
- Pearson, C., Murphy, J. & Hermes, R., 1986. Acoustic and resistivity measurements on rock samples containing tetrahydrofuran hydrates: laboratory analogues to natural gas hydrate deposits, *J. geophys. Res.*, **91**, 14 132–14 138.
- Pecher, I.A., Holbrook, W.S., Sen, M.K., Lizarralde, D. & Wood, W.T., 2003. Seismic anisotropy in gas-hydrate- and gas-bearing sediments on the Blake Ridge, from a walk away vertical seismic profile, *Geophys. Res. Lett.*, **30**, 1733, doi:10.1029/2003GL017477.
- Rider, M.H., 1996. *The Geological Interpretation of Well Logs*, Whittles Publishing, Caithness.
- Sakai, A., 1999. Velocity analysis of vertical seismic profile (VSP) survey at JAPEx/JNOC/GSC Mallik 2L-38 gas hydrate research well, and related problems for estimating gas hydrate concentration, in *Scientific Results From JAPEx/JNOC/GSC Mallik 2L-38 Gas Hydrate Research Well, Mackenzie Delta, Northwest Territories, Canada*, Geological Survey of Canada Bulletin 544, pp. 323–340, eds Dallimore, S.R., Uchida, T. & Collett, T.S., Geological Survey of Canada, Ottawa, Canada.
- Santos, J.E., Corbero, J. & Douglas, J. Jr, 1990a. Static and dynamic behaviour of a porous solid saturated by a two-phase fluid, *J. acoust. Soc. Am.*, **87**, 1428–1438.
- Santos, J.E., Douglas, J. Jr, Corbero, J. & Lovera, O.M., 1990b. A model for wave propagation in a porous medium saturated by a two-phase fluid, *J. acoust. Soc. Am.*, **87**, 1439–1448.
- Sassen, R. & MacDonald, I.R., 1994. Evidence for structure H hydrate, Gulf of Mexico continental slope., *Org. Geochem.*, **22**, 1029–1032.
- Sheng, P., 1990. Effective-medium theory of sedimentary rocks, *Phys. Rev. B*, **41**, 4507–4512.
- Shipley, T.H., Houston, M., Buffler, R.T., Shaub, F.J., McMillan, K.J., Ladd, J.W. & Worzel, J.L., 1979. Seismic reflection evidence for the wide-spread occurrence of possible gas-hydrate horizons on continental slopes and rises, *Am. Assoc. Petrol. Geol. Bull.*, **63**, 2204–2213.
- Singh, S.C., Minshull, T.A. & Spence, G.D., 1993. Velocity structure of a gas hydrate reflector, *Science*, **260**, 204–207.
- Sloan, E.D., 1990. *Clathrate Hydrates of Natural Gas*, Marcel Dekker, New York.
- Stoll, R.D. & Bryan, G.M., 1979. Physical properties of sediments containing gas hydrates, *J. geophys. Res.*, **84**, 1629–1634.
- Stoll, R.D., Ewing, J. & Bryan, G.M., 1971. Anomalous wave velocities in sediments containing gas hydrates, *J. geophys. Res.*, **76**, 2090–2094.
- Tinivella, U. & Accaino, F., 2000. Compressional velocity structure and Poisson's ratio in marine sediments with gas hydrate and free gas by inversion of reflected and refracted seismic data (South Shetland Islands, Antarctica), *Mar. Geol.*, **164**, 13–27.
- Tinivella, U. & Lodolo, E., 2000. The Blake Ridge bottom-simulating reflector transect: tomographic velocity field and theoretical model to estimate methane hydrate quantities, in *Proceedings of the Ocean Drilling Program, Scientific Results 164*, pp. 273–281, eds Paull, C.K., Matsumoto, R., Wallace, P.J. & Dillon, W.P., Ocean Drilling Program, College Station, TX.
- Todd, T. & Simmons, G., 1972. Effect of pore pressure on the velocity of compressional waves in low-porosity rocks, *J. Geophys. Res.*, **77**, 3731–3743.
- Uchida, T., Matsumoto, R., Waseda, A., Okui, T., Yamada, K., Uchida, T., Okada, S. & Takano, O., 1999. Summary of physicochemical properties of natural gas hydrate and associated gas-hydrate-bearing sediments, JAPEx/JNOC/GSC Mallik 2L-38 gas hydrate research well, by the Japanese research consortium, in *Scientific Results From JAPEx/JNOC/GSC Mallik 2L-38 Gas Hydrate Research Well, Mackenzie*

- Delta, Northwest Territories, Canada*, Geological Survey of Canada Bulletin 544, pp. 205–228, eds Dallimore, S.R., Uchida, T. & Collett, T.S., Geological Survey of Canada, Ottawa, Canada.
- Waite, W.F., Helgerud, M.B., Nur, A., Pinkston, J.C., Stern, L.A., Kirby, S.H. & Durham, W.B., 1998. First laboratory measurements of compressional and shear wave speeds through pure methane hydrate, in 3rd International Conference on Gas Hydrates, *Ann. NY Acad. Sci.*, **912**, 1003–1010.
- Walia, R., Mi, Y., Hyndman, R.D. & Sakai, A., 1999. Vertical seismic profile (VSP) in the JAPEX/JNOC/GSC Mallik 2L-38 gas hydrate research well, in *Scientific Results From JAPEX/JNOC/GSC Mallik 2L-38 Gas Hydrate Research Well, Mackenzie Delta, Northwest Territories, Canada*, Geological Survey of Canada Bulletin 544, pp. 341–355, eds Dallimore, S.R., Uchida, T. & Collett, T.S., Geological Survey of Canada, Ottawa, Canada.
- Willis, J.R., 1977. Bounds and self-consistent estimates for the overall properties of anisotropic composites, *J. Mech. Phys. Solids*, **25**, 185–202.
- Winters, W.J. *et al.*, 1999. Physical properties of sediments from the JAPEX/JNOC/GSC Mallik 2L-38 gas hydrate research well, in *Scientific Results From JAPEX/JNOC/GSC Mallik 2L-38 Gas Hydrate Research Well, Mackenzie Delta, Northwest Territories, Canada*, Geological Survey of Canada Bulletin 544, pp. 95–100, eds Dallimore, S.R., Uchida, T. & Collett, T.S., Geological Survey of Canada, Ottawa, Canada.
- Winters, W.J., Dillon, W.P., Pecher, I.A. & Mason, D.H., 2000. GHASTLI—determining physical properties of laboratory hydrate, in *Natural Gas Hydrate in Oceanic Permafrost Environments, Coastal Systems and Continental Margins*, Vol. 5, pp. 317–322, ed. Max, M.D., Kluwer, Dordrecht.
- Wood, A.B., 1941. *A Textbook of Sound*, Macmillan, New York.
- Wood, W.T. & Ruppel, C., 2000. Seismic and thermal investigations of the Blake Ridge gas hydrate area: A synthesis, in *Proceedings of the Ocean Drilling Program, Scientific Results 164*, pp. 253–264, eds Paull, C.K., Matsumoto, R., Wallace, P.J. & Dillon, W.P., Ocean Drilling Program, College Station, TX.
- Wyllie, M.R., Gregory, A.R. & Gardener, G.H.P., 1958. An experimental investigation of factors affecting elastic wave velocities in porous media, *Geophysics*, **23**, 459–493.
- Xu, S. & White, R., 1995. A new velocity model for clay-sand mixtures, *Geophys. Prospect.*, **43**, 91–118.
- Xu, Y. & Chopra, S., 2003. Possibility of AVI applications in gas hydrate exploration in Mackenzie Delta, Canada, in *73rd Annual Meeting of the Society of Exploration Geophysicists, Dallas, Texas*, Paper AVOP1-AVO I-5, pp. 258–261. Society of Exploration Geophysicists, New York.
- Zimmerman, R.W. & King, M.S., 1986. The effect of the extent of freezing on seismic velocities in unconsolidated permafrost, *Geophys.*, **39**, 587–606.